Insights in the chemical components of liposomes responsible for P-glycoprotein inhibition.

Insights in the chemical components of liposomes responsible for P-glycoprotein inhibition

Joanna Kopecka [1,*], Msc, PhD, Giuseppina Salzano [2,*], PharmD, Ivana Campia [1], Msc, Sara Lusa [2], Dario Ghigo [1], MD, Giuseppe De Rosa [2,#], PhD, Chiara Riganti [1,#], MD

[1]Department of Oncology, Università di Torino, via Santena 5/bis, 10126 Torino (Italy)

[2]Department of Pharmacy, Università degli Studi di Napoli Federico II, Via D. Montesano 49, 80131 Napoli (Italy)

[*] Both authors contributed equally to this work

[#] Both authors contributed equally to this work

Short title: PEGylated neutral liposomes inhibit P-glycoprotein

Corresponding authors: Dr. Chiara Riganti, Department of Oncology, Università di Torino, via Santena 5/bis, 10126, Torino (Italy), phone: +390116705857, fax: +390116705845, email: chiara.riganti@unito.it; Dr. Giuseppe De Rosa, Department of Pharmacy, Università degli Studi di Napoli Federico II, Via D. Montesano 46, 80131 Naples (Italy), phone: +39081678666, fax: +39081678630, e-mail: gderosa@unina.it

Conflict of interest

There are no disclosures or any conflict of interests.

Funding

This work was supported with funds from Compagnia di San Paolo “Programma Neuroscienze”, Italy (grant 2008.1136 to CR); Italian Association for Cancer Research (MFAG 11475 to CR); Italian Ministry of University and Research (PRIN 2009 to GD; Program “Future in Research” FIRB 2012, grant RBFR12SOQ1 to CR).

Joanna Kopecka is the recipient of a “Mario and Valeria Rindi” fellowship from Italian Foundation for Cancer Research (FIRC).

Word count:

Abstract: 149

Manuscript: 4868

Number of Figures: 6

Number of Tables: 1

Abstract

In this work we investigated how the surface charge and the presence of polyethylene glycol (PEG) on liposome carriers affect the delivery of the encapsulated doxorubicin in P-glycoprotein (Pgp)-overexpressing cells.

We found that neutral net charge was critical to favour the liposome uptake and decrease the Vmax of doxorubicin efflux. PEG-coating was necessary to increase the Km of doxorubicin for Pgp. In particular the PEGylated phospholipid present in neutral liposomes, i.e. PEGylated distearoyl-phosphatidylethanolammine (DSPE-PEG), was a Pgp allosteric inhibitor, increased doxorubicin Km and inhibited Pgp ATPase activity. Site-directed mutagenesis experiments suggested that the domain centred around glycine 185 of Pgp was necessary for these inhibitory properties of DSPE-PEG and PEGylated neutral liposomes.

We conclude that both surface charge and PEGylation must be considered to optimize the doxorubicin delivery within chemoresistant cells. DSPE-PEG-enriched particles may represent promising tools for therapeutic and diagnostic applications in tissues with high levels of Pgp.

Keywords: liposome, doxorubicin, P-glycoprotein, polyethylene glycol, chemoresistance

Background

Doxorubicin was one of the first drugs encapsulated within liposomes and liposomal doxorubicin (Doxyl/Caelyx) is actually approved for the treatment of metastatic and drug-resistant breast and ovary cancers [1]. The greater drug delivery within the tumor core due to the enhanced permeability and retention effect [2], the possibility of co-encapsulating more than one drug, e.g. a chemotherapeutic drug and a chemosensitizer [3], or a chemotherapeutic drug and a gene therapy-tool [4,5], may explain the success of liposomes in the fight against resistant cancers.

Liposomal drugs seem also less susceptible than free drugs to the efflux activity by ATP-binding cassette transporters, such as P-glycoprotein (Pgp/ABCB1), multidrug-resistance related proteins (MRPs/ABCCs) and breast cancer resistance protein (BCRP/ABCG2) [2,6,7]. Liposomal drugs ensure a more prolonged release of the drug within tumor cells, since they are less potent inducers of Pgp than free drugs [8], or directly interfere with Pgp activity [6,7]. We previously showed that liposomal doxorubicin inhibits the activity of Pgp [9], by interacting with a domain overlapping with one of the drug-releasing sites [10]. Since it is unlikely that whole liposomes interact with the protein, we hypothesize that the inhibitory effects on Pgp are produced by a single lipid component or by a lipid-associated form of doxorubicin released from the liposomes.

Aim of this work is to investigate which are the critical liposome features – in terms of surface charge, phospholipids composition, polyethylene glycol (PEG) coating – that impair the activity of Pgp, in order to optimize the design of liposomal drugs with Pgp-inhibitory properties. We prepared different formulations of liposomal doxorubicin with controlled size, with different surface net charge, with or without PEG, with or without cholesterol, and we

tested their efficacy in the doxorubicin-sensitive breast cancer MCF7 cells and in their Pgp-overexpressing (Pgp+) doxorubicin-resistant counterpart (MCF7-dx).

Methods

Liposome preparation and characterization. Liposomes with different lipid compositions were prepared (see Supplementary materials for details). The mean diameter of liposomes was determined by photon correlation spectroscopy (N5, Beckman Coulter, Miami, USA). Each sample was diluted in deionizer/filtered (0.22 μm pore size, polycarbonate filters, MF-Millipore, Billerica, MA) water and analyzed with detector at 90° angle. Polydispersity index (P.I.) was used as measure of the particle size distribution. The zeta-potential (ζ) of liposomes was determined by means of a Zetasizer Nano Z (Malvern, UK).

For doxorubicin loading, 1.5 mmol/L doxorubicin in sterile aqueous solution was added to each liposome preparation. The residual non-encapsulated drug was removed by gel filtration in a Sephadex G-50 (Amersham Bioscience, Piscataway, NJ, USA) column. The liposomes were stored at 4°C, diluted at a doxorubicin concentration of 0.5 mmol/L and used in the subsequent experiments. The amount of encapsulated doxorubicin was quantified by diluting 50 μL of liposomal suspension in 0.5 mL of 1:1 v/v ethanol/HCl 0.3 N, sonicating the liposomes (2 bursts of 10 sec, amplitude 40%, with a Hielscher UP200S ultrasound sonicator, Hielscher Ultrasonics GmbH, Teltow, Germany) and measuring the fluorescence emitted by the drug with a LS-5 spectrofluorimeter (PerkinElmer, Waltham, MA). Excitation and emission wavelengths were 475 nm and 553 nm respectively. The encapsulation efficiency was calculated as ratio between the percentage of the actual doxorubicin encapsulated and the percentage of the expected doxorubicin encapsulated.

Cells. Human doxorubicin-sensitive breast cancer MCF7 cells and Pgp+ doxorubicin resistant MCF7-dx cells were cultured in RPMI 1640 medium, supplemented with 10% v/v foetal bovine serum, 1% v/v penicillin-streptomycin and 1% v/v L-glutamine. To generate the Pgp+ MCF7-dx cells, the pHa vector containing the complete *mdr1* cDNA was purchased from Addgene (Cambridge, MA) and subcloned into pCDNA3 vector (Invitrogen Life Technologies, Milan, Italy) as described [11]. By sequencing the *mdr1* gene present in the pCDNA3 vector, we verified that it contained the codon GGA (nucleotides 553-555), codifying for glycine at position 185 of the protein (data not shown). As shown in the Supplementary Figure 1, MCF7 cells did not express detectable amounts of Pgp and MRP1 and had a very low amount of BCRP; Pgp+ MCF7-dx cells had the same pattern of MRP1 and BCRP expression exhibited by MCF7 cells, and a high level of Pgp.

Intracellular doxorubicin accumulation. The intracellular accumulation of doxorubicin was detected spectrofluorimetrically, as described [12]. Fluorescence was converted into nmol doxorubicin/mg cell proteins using a calibration curve prepared previously.

Doxorubicin uptake. Cells were incubated at 37°C with 1 μmol/L free doxorubicin or liposomal doxorubicin formulations; at t_0 and fixed time points (up to 20 min), cells were washed five times with PBS, detached with trypsin/EDTA, centrifuged at 13,000 x g for 5 min, re-suspended in 1:1 v/v ethanol/HCl 0.3 N, and checked for the intracellular doxorubicin, taken as an index of the drug uptake. Fluorescence was converted into nmol doxorubicin/mg cell proteins using a calibration curve prepared previously. The "uptake benefit" was calculated by dividing the fluorescence of cells incubated for 20 min with each liposomal formulation by the fluorescence of cells incubated with free doxorubicin after the same time period. The liposomes intracellular distribution was performed by confocal microscope as detailed in the Supplementary Materials.

Doxorubicin efflux. Cells were incubated at 37°C for 10 min with 1 μmol/L doxorubicin or liposomal doxorubicin formulations, then washed five times with PBS and rinsed with 1 mL fresh PBS. Aliquots of extracellular supernatant were collected at t_0 and fixed time points (up to 20 min), and checked for the doxorubicin amount. Fluorescence was converted into nmol doxorubicin/mg cell proteins using a calibration curve prepared previously. The "efflux benefit" was calculated by dividing the fluorescence of supernatants collected from cells for 20 min with free doxorubicin by the fluorescence of supernatants collected from cells incubated with each liposomal formulation after the same time period.

Kinetic parameters were calculated as previously reported [12]. Values were fitted to Michaelis-Menten equation to calculate Vmax and Km, using the Enzfitter software (Biosoft Corporation, Cambridge, United Kingdom).

ATPase assay. The assay was performed on Pgp-rich membrane vesicles as described in [9]. The ATPase activity was expressed as μmol hydrolyzed phosphate/min/mg cell proteins, according to the titration curve previously prepared.

Verapamil and colchicine binding. Pgp-rich membrane vesicles containing 10 μg proteins were incubated in MultiScreen 96-wells plate 0.22 μm pore-size (Millipore) for 30 min at room temperature with 1.2 nmol/L [^{3}H]-verapamil, 1 nmol/L [^{3}H]-colchicine or 1 nmol/L [^{3}H]-vinblastine, in the absence or presence of different concentrations of doxorubicin, DSPE-PEG or cold ligands. Binding assay was performed as previously reported [9].

Site-directed mutagenesis. pCDNA3 vector containing the wild-type *mdr1* cDNA, was subjected to PCR-based mutagenesis using the QuikChange kit (Stratagene, La Jolla, CA), following the manufacturer's instructions. The nucleotides at positions 554 and 555 were

mutated from GA to TT, yielding the codon GTT (encoding for valine at position 185 in Pgp protein). The mutation was confirmed by DNA sequencing (data not shown).

Statistical analysis. All data in text and figures are provided as mean ± SD. The results were analyzed by a one-way analysis of variance (ANOVA) and Tukey's test. $p<0.05$ was considered significant.

Results

Liposomes characterization

Liposome formulations with different lipid composition were prepared (Table 1). Liposomes had a mean size ranging from about 125 to about 150 nm, with a P.I. in all cases lower than 0.2. The lipid composition was selected in order to have liposomes with significantly different ζ; thus, liposomes containing 1,2-dipalmitoyl-*sn*-glycero-3-phospho-rac-glycerol (DPPG) characterized by a net negative charge between -40 and -63 mV were considered "anionic liposomes"; liposomes containing 1,2-dioleoyloxy-3-trimethylammoniumpropanchloride (DOTAP) with a net positive charge of about +30 mV were considered "positive liposomes"; liposomes based on only 1,2-dipalmitoyl-*sn*-glycero-3-phosphocholine (DPPC) characterized by a moderate negative net charge were considered, in comparison with the other formulations, "neutral liposomes". In all cases, the presence of PEGylated lipids shielded the net surface charge (Table 1).

The actual loading of doxorubicin for each liposomal formulation is reported in Table 2. For all formulations the mean encapsulation efficiency was higher than 80%, without significant differences between non PEGylated and PEGylated liposomes, liposomes with different surface charge or different amount of lipids and DPPC (Table 2).

Different liposomal doxorubicin formulations show different patterns of intracellular accumulation

MCF7 and Pgp+ MCF7-dx cells were incubated for 24 h with increasing concentrations of free doxorubicin and anionic, neutral or cationic liposomal doxorubicin, either non PEGylated (Figure 1A-B) or PEGylated (Figure 1C-D). Free doxorubicin and liposomal doxorubicin formulations accumulated within MCF7 cells in a dose-dependent way; no significant differences were detected between liposomal doxorubicin and free doxorubicin, or among the liposomal formulations (Figure 1A and 1C). In MCF7-dx cells, free doxorubicin had a lower intracellular accumulation (Figure 1B); the rank order of intracellular doxorubicin retention was: neutral liposomal doxorubicin > anionic liposomal doxorubicin > cationic liposomal doxorubicin = free doxorubicin (Figure 1B). PEGylated liposomes were more effective than the corresponding non-PEGylated ones (Figure 1D).

MCF7 and Pgp+ MCF7-dx cells were then incubated with 1 μM free doxorubicin and liposomal doxorubicin formulations, non PEGylated (Figure 1E-F) or PEGylated (Figure 1G-H), for different time periods. As expected, doxorubicin showed a time-dependent accumulation, higher in MCF7 than in MCF7-dx cells. Again, the rank order of intracellular doxorubicin accumulation was: neutral liposomal doxorubicin > anionic liposomal doxorubicin > cationic liposomal doxorubicin = free doxorubicin, in both MCF7 (Figure 1E) and MCF7-dx cells (Figure 1F).

PEGylated neutral liposomes was the most effective formulation for doxorubicin delivery and yielded the same intracellular drug accumulation in MCF7 and MCF7-dx cells (Figure 1G-H).

Surface charge and PEGylation of liposomes affect the kinetics of doxorubicin uptake and efflux from Pgp+ MCF7-dx cells

In MCF7-dx cells neutral liposomal doxorubicin, either non PEGylated (Figure 2A**)** or PEGylated (Figure 2B), was more promptly uptaken than anionic and cationic liposomal doxorubicin or free doxorubicin, and was the only liposomal formulation showing a significant advantage in the uptake compared with free doxorubicin (Figure 2C). Such advantage was abrogated if the uptake assay was performed at 4°C instead of 37°C (Supplementary Figure 2).

Confocal microscopy images also showed a different distribution of fluorescently labelled liposomes, depending on the lipid composition. In the case of anionic and cationic liposomes (Supplementary Figure 3A and 3C) the lipid-associated fluorescence (green) appeared non-uniformly distributed in the cells. In the case of neutral liposomes (Supplementary Figure 3B) the green fluorescence was homogeneously distributed in the cytoplasm. The use of PEGylated liposomal formulations produced in all cases a more diffuse cytosolic distribution when compared to non PEGylated ones (Supplementary Figure 4).

Doxorubicin encapsulated into liposomes was less extruded from Pgp+ MCF7-dx cells than free doxorubicin: in particular neutral liposomal doxorubicin was less effluxed than anionic liposomal doxorubicin, which was in turn less effluxed than cationic liposomal doxorubicin (Figure 2D). If we compare the non PEGylated (Figure 2D) and the PEGylated (Figure 2E) liposomal formulations with the same surface charge, the rate of doxorubicin efflux was lower with the latter. As summarized in Figure 2F, the relative benefit in the efflux process was: PEGylated neutral liposomal doxorubicin > neutral liposomal doxorubicin > PEGylated anionic liposomal doxorubicin > anionic liposomal doxorubicin > PEGylated cationic liposomal doxorubicin = cationic liposomal doxorubicin = free doxorubicin.

The efflux rate of free and liposomal doxorubicin formulations from Pgp+ MCF7-dx cells followed a first order kinetics (Figure 2G). All liposomal formulations had a higher Km than

free doxorubicin; neutral liposomal doxorubicin also had a lower Vmax (Figure 2G). Surprisingly, PEGylation dramatically increased the Km, producing minor effects on Vmax (Figure 2H). Of note, the kinetics of efflux became sigmoidal, suggesting that PEGylated formulations may act as negative allosteric modulators of doxorubicin efflux. Again, the most pronounced effects were obtained with the PEGylated neutral liposomal formulation, followed by the anionic and the cationic ones (Figure 2H).

Neutral PEGylated liposomal doxorubicin impairs the Pgp ATPase activity

The verapamil-induced ATPase activity of Pgp, taken as index of the maximal transporter activity, was not affected by free doxorubicin, cationic or anionic liposomal doxorubicin, but it was reduced by neutral liposomal doxorubicin (Figure 3A). The PEGylation made the liposomal formulations stronger inhibitors of Pgp, with this rank order: neutral liposomal doxorubicin > anionic liposomal doxorubicin > cationic liposomal doxorubicin (Figure 3B). The rate of ATP hydrolysis in the absence of verapamil, taken as an index of the basal activity of Pgp, was also measured: again, non PEGylated formulations (Figure 3C) were weaker inhibitors than PEGylated ones (Figure 3D). The PEGylated neutral liposomes were the most effective inhibitors (Figure 3D).

PEGylated distearoyl-phosphatidylethanolammine (DSPE-PEG) is an allosteric inhibitor of Pgp

Since the strongest inhibition of Pgp activity was achieved with PEGylated liposomes, we next investigated the effects of PEG and PEGylated phospholipid (DSPE-PEG) present in our liposomal formulations on the transporter. PEG alone significantly reduced both the verapamil-induced (Figure 4A) and the basal (Figure 4B) ATPase activity of Pgp; DSPE-PEG exerted an even stronger effect on ATPase activity. This effect was preserved also when

DSPE-PEG was co-incubated with free doxorubicin, which *per se* did not change the activity of Pgp (Figure 4A-B). When the efflux of doxorubicin was measured in Pgp+ MCF7-dx cells treated with the association of DSPE-PEG and doxorubicin, the Km of doxorubicin was dramatically reduced (Figure 4C) and the kinetic parameters of its efflux became similar to those observed with PEGylated neutral liposomal doxorubicin (Figure 2H).

The presence of cholesterol does not affect doxorubicin uptake, efflux, kinetic parameters and ATPase activity of Pgp

The presence of cholesterol may affect the physic-chemical properties of the liposomes, e.g. by changing the liposomal envelope fluidity and eventually affecting the interaction between liposomes and plasma membrane. To clarify the role of cholesterol in our formulations, we produced cholesterol-free neutral liposomes, either PEGylated or not. The cholesterol-free formulations did not show significantly different properties from the corresponding cholesterol-containing ones, in terms of doxorubicin uptake (Supplementary Figure 5A), doxorubicin efflux (Supplementary Figure 5B), kinetic parameters (Supplementary Figure 5C), verapamil-induced (Supplementary Figure 5D) and basal (Supplementary Figure 5E) ATPase activity. These data suggest that in our model the role of cholesterol in the liposomal envelope is not relevant.

DSPE-PEG interferes with Pgp activity by binding the verapamil/colchicine binding site

In competition binding assays with known ligands of Pgp, we found that DSPE-PEG displaced [^{3}H]-verapamil, showing the same displacement profile of cold verapamil (Figure 5A). DSPE-PEG also interfered with the binding of [^{3}H]-colchicine; in this case the displacement profile differed from that of cold colchicine (Figure 5B). The displacement of [^{3}H]-verapamil and [^{3}H]-colchicine occurred also when DSPE-PEG was co-incubated with

doxorubicin, which did not interfere with the binding of the other compounds at each concentration tested (Figure 5A-B). The binding of other ligands, like [^{3}H]-vinblastine, was not affected by DSPE-PEG (data not shown).

These data suggest that DSPE-PEG may interact with Pgp on a putative site binding verapamil and colchicine.

The G185V-mutated Pgp displays an altered binding of verapamil and colchicine [13] and is not sensitive to the effects of liposomal doxorubicin [9]. To verify whether the domain containing glycine 185 was the putative binding site of DSPE-PEG, we transfected MCF7 cells with the wild-type and the G185V-mutated Pgp expression vectors. Both proteins were expressed at the same level (Figure 6A) and induced a significant reduction of the intracellular doxorubicin (Figure 6B). Whereas DSPE-PEG strongly increased the doxorubicin retention in wild-type Pgp+ MCF7-dx cells, it did not in G185V Pgp+ MCF7-dx cells (Figure 6B). G185V Pgp had the same affinity for verapamil (Figure 6C) and a higher affinity for colchicine (Figure 6D) than wild-type Pgp (Figure 5A-B). No displacement of [^{3}H]-verapamil (Figure 6C) or [^{3}H]-colchicine (Figure 6D) was achieved by DSPE-PEG on G185V Pgp. In addition, DSPE-PEG did not reduce the ATPase activity of G185V Pgp, either after stimulation with verapamil (Figure 6E) or in basal condition (Figure 6F). Also the whole PEGylated neutral liposomal particles were devoid of any inhibitory effect on G185V Pgp (Figure 6E-F).

Discussion

To investigate which surface features (i.e. charge, presence of PEG coating) of liposomes are necessary to reduce the activity of Pgp, we produced doxorubicin-encapsulating liposomes with different lipid composition, i.e. with anionic, neutral or cationic surface net charge, with or without PEGylated lipids, with or without cholesterol. We tested them in the doxorubicin-

sensitive MCF7 cells and in the Pgp+ doxorubicin-resistant MCF7-dx cells, chosen as a model of cells with high expression of Pgp and low or undetectable amount of the other transporters involved in the doxorubicin efflux (MRP1 and BCRP). Optimizing the design of liposomes with Pgp-inhibitory properties is worthy of investigations in drug-resistant breast cancers, because PEGylated liposomal doxorubicin (Doxyl/Caelyx) is currently used in these tumors, but therapeutic success is not obtained in all patients [1].

In our model of Pgp+ cells, the most effective doxorubicin delivery was achieved by neutral liposomes, in particular PEGylated ones. Depending on the cell model and pattern of charged glycoproteins and glycolipids present in plasma membrane, differently charged liposomes may be more or less favored to enter within the cell [14,15]. Differently charged particles also follow different pathways of endocytosis [16]: for instance, the most easily uptaken nanoparticles in brain microvascular endothelial cells at 37°C are the neutral and anionic ones. At 4°C, when active endocytosis is blunted, they are not detected within cells but only in proximity of cells surface [16]. This situation is in keeping with our results in Pgp+ MCF7-dx cells, where neutral liposomes were the most promptly uptaken, likely by a process of endocytosis, since no uptake was detected at 4°C. The presence of PEG did not confer any significant advantage in the uptake.

The interaction of cationic lipids with specific cell components, i.e. anionic lipids, has been proposed as a mechanism that triggers the rapid release of nucleic acid from lipoplexes [17,18]. We can speculate that the same rapid release – subsequent to the disassembly of the liposomal shell within the cell – may occur for doxorubicin carried by cationic liposomes: once returned in the form of free doxorubicin, the drug is easily recognized by Pgp and pumped outside. Indeed, doxorubicin encapsulated in cationic liposomes was as effluxed as free doxorubicin by Pgp+ MCF7-dx cells. Interestingly, recent studies on the intracellular distribution showed

that charged liposomes usually form large aggregates [19]; such pattern is suggestive of liposomal disassembly and cargo release within the cell. Pgp+ MCF7-dx cells treated with anionic and cationic liposomes showed indeed a punctuate and non-uniform distribution; by contrast, neutral liposomes had a homogeneously distributed green fluorescence in the cytoplasm. Of note, the presence of PEG, irrespectively of the net charge surface, produced the same uniform distribution, which is index of higher stability of the nanocarriers and slower release of the cargo. This feature is expected to ensure a lower efflux of the drug via Pgp and led us to investigate how doxorubicin encapsulated in different liposomal formulations was extruded from Pgp+ MCF7-dx cells.

Unexpectedly, neutral liposomes decreased the Vmax of doxorubicin efflux from Pgp+ cells, acting as non-competitive inhibitors of Pgp. Such inhibition could be due to an unfavoured conformation of Pgp, e.g. produced by changes in the lipids environment. Pgp is strongly affected by the lipids microenvironment [20]; small changes in lipids composition produce dramatic variations in the pump's activity [21,22]. The absence of a net surface charge may favor the interaction of neutral liposomes, more than anionic or cationic ones, with the plasma membrane where Pgp is embedded. The most striking effects on doxorubicin efflux, however, were achieved by PEGylated liposomes, which all significantly increased the Km of doxorubicin and acted as allosteric inhibitors. The strongest inhibition on the catalytic activity of Pgp and doxorubicin transport was achieved by neutral PEGylated liposomes, which simultaneously reduced the Vmax and increased the Km.

Few evidences of the benefits of PEG-nanocarriers in Pgp-overexpressing cells have been reported [23,24,25]. For instance rhodamine 123 was more retained within MCF7-dx cells if loaded in PEGylated liposomes than in non-PEGylated ones [26]. In this case, the presence of cholesterol in the liposomal envelope was critical, because it makes the lipid shell more rigid,

preventing the release of rhodamine from liposomes [26]. In our model no difference was detected between neutral liposomes with or without cholesterol, suggesting that the mechanism hypothesized for rhodamine was of secondary importance for doxorubicin. In other models, the benefits of PEG were attributed to changes in membrane fluidity [27] or to down-regulation of Pgp mRNA. This effect was evident however at 30 µmol/L concentration [25]. Of note, PEG 2000 – the same molecule used in our PEgylated formulations – was reported as the most effective type of PEG in Pgp-expressing cells [28]. In our hands, DSPE-PEG was more potent than PEG alone in reducing the ATPase activity of Pgp, being effective already at 100 nmol/L. Interestingly, Pgp showed an increased Km for doxorubicin co-administrated with DSPE-PEG, suggesting that DSPE-PEG may impair the binding of doxorubicin to Pgp. The displacement assays showed that DSPE-PEG directly competed with verapamil and interfered with colchicine for the binding to Pgp; these data indicate that DSPE-PEG likely interacts with the verapamil/colchicine binding site, a domain centered around glycine 185 [13]. Indeed in G185V Pgp+ MCF7-dx cells DSPE-PEG completely lost its efficacy, in terms of doxorubicin retention, verapamil/colchicine displacement and Pgp inhibition, suggesting that DSPE-PEG did not interact with this mutant Pgp.

The glycine 185-centered domain is important for the drug release towards the extracellular environment [10] and for the transmission of the conformational changes induced by substrates to the catalytic site of Pgp [29]. We propose that, by interacting with this domain, DSPE-PEG exerts an allosteric inhibition, interferes with the catalytic cycle of Pgp and the transport of substrates.

Overall our results suggest that two critical features, in order to achieve the maximal doxorubicin accumulation within Pgp-overexpressing cells, are: 1) the liposomal neutral surface, which favors the liposome uptake and stability; 2) the presence of DSPE-PEG, which

directly inhibits Pgp. After entering within the cell, the liposomal envelope is gradually disrupted, and releases doxorubicin and DSPE-PEG: since DSPE-PEG prevents the efflux of doxorubicin, liposomes containing DSPE-PEG are the most suitable to increase the intracellular retention of doxorubicin in Pgp-overexpressing cells. This work paves the way to the future validations of PEG-based nanocarriers, as potential therapeutic and diagnostic tools optimized for tissues with high levels of Pgp, such as drug-resistant tumors or physiological barriers, like blood-brain barrier and blood-placental barrier.

Acknowledgments

We are grateful to Costanzo Costamagna (Department of Oncology, Università di Torino) for the technical assistance provided.

References

1. Markman M. Pegylated liposomal doxorubicin in the treatment of cancers of the breast and ovary. Expert Opin Pharmacother 2006;**7**:1469-74.

2. Jabr-Milane LS, van Vlerken LE, Yadav S, Amiji MM. Multi-functional nanocarriers to overcome tumour drug resistance. Cancer Treat Rev 2008;**34**:592-602.

3. Patel NR, Rathi A, Mongayt D, Torchilin VP. Reversal of multidrug resistance by co-delivery of tariquidar (XR9576) and paclitaxel using long-circulating liposomes. Int J Pharm 2011;**416**:296-99.

4. Chen Y, Bathura SR, Li J, Huang L. Multifunctional nanoparticles delivering small interfering RNA and doxorubicin overcome drug resistance in cancer. J Biol Chem 2010;**285:**22639-50.

5. Guo L, Fan L, Pang Z, Ren J, Ren Y, Li J, et al. TRAIL and doxorubicin combination enhances anti-glioblastoma effect based on passive tumor targeting of liposomes. J Control Release 2011;**154**:93-102.
6. Rahman A, Husain SR, Siddiqi J, Verma M, Agresti M, Center M, et al. Liposome-mediated modulation of multidrug resistance in human HL-60 leukemia cells. J Natl Cancer Inst 1992;**84**:1909-15.
7. Thierry AR, Dritschilo A, Rahman A. Effect of liposome on P-glycoprotein function in multidrug-resistant cells. Biochem Biophys Res Commun 1992;**187**:1098-105.
8. Zalipsky S, Saad M, Kiwan R, Ber E, Yui N, Minko T. Antitumor activity of new liposomal prodrug of mitomycin C in multidrug resistant solid tumors. Insights of the mechanism of action. J Drug Target 2007;**15**:518-30.
9. Riganti C, Voena C, Kopecka J, Corsetto P, Montorfano G, Enrico E, et al. Liposome-encapsulated doxorubicin reverses drug-resistance by inhibiting P-glycoprotein in human cancer cells. Mol Pharm 2011;**8**:683-700.
10. Safa AR, Sterns RK, Choi K, Agresti M, Tamai I, Metha ND, et al. Molecular basis of preferential resistance to colchicine in multidrug-resistant human cells conferred by Gly-185 Val-185 substitution in P-glycoprotein. Proc Natl Acad Sci USA 1990;**87**:7225-29.
11. Doublier S, Riganti C, Voena C, Costamagna C, Aldieri E, Pescarmona G, et al. RhoA silencing reverts the resistance to doxorubicin in human colon cancer cells. Mol Cancer Res 2008;**6**:1607-20.
12. Riganti C, Miraglia E, Viarisio D, Costamagna C, Pescarmona G, Ghigo D, et al. Nitric Oxide reverts the resistance to doxorubicin in human colon cancer cells by inhibiting the drug efflux. Cancer Res 2005;**65**:516-25.

13. Rao US. Mutation of glycine 185 to valine alters the ATPase function of the human P-glycoprotein expressed in Sf9 cells. J Biol Chem 1995;**270**:6686-90.

14. Lockman PR, Koziara JM, Mumper RJ, Allen DD. Nanoparticle surface charges alter blood-brain barrier integrity and permeability. J Drug Target 2004;**12**:635-41.

15. Dadashzadeh S, Mirahmadi N, Babaei MH, Vali AM. Peritoneal retention of liposomes: effects of lipid compostion, PEG coating and liposome charge. J Control Release 2010;**148**:177-86.

16. Jallouli Y, Paillard A, Chang J, Sevin E, Betbeder D. Influence of surface charge and inner composition of porous nanoparticles to cross blood-brain barrier in vitro. Int J Pharm 2007;**344**:103-09.

17. Zelphati O, Szoka FC Jr. Mechanism of oligonucleotide release from cationic liposomes. Proc Natl Acad Sci USA 1996;**93**:11493-98.

18. Marcusson EG, Bhat B, Manoharan M, Bennett CF, Dean NM. Phosphorothioate oligodeoxyribonucleotides dissociate from cationic lipids before entering the nucleus. Nucleic Acids Res **1998**; 26:2016-23.

19. Chernenko T, Sawant RR, Miljkovic M, Quintero L, Diem M, Torchilin V. Raman microscopy for noninvasive imaging of pharmaceutical nanocarriers: intracellular distribution of cationic liposomes of different composition. Mol Pharm 2012;**9**:930-36.

20. Gayet L, Dayan G, Barakat S, Labialle S, Michaud M, Cogne S, et al. Control of P-glycoprotein activity by membrane cholesterol amounts and their relation to multidrug resistance in human CEM leukemia cells. Biochemistry 2005; **44**:4499-09.

21. Barta CA, Sachs-Barrable K, Feng F, Wasan KM. Effects of monoglycerides on P-glycoprotein: modulation of the activity and expression in Caco-2 cell monolayers. Mol Pharm 2008; **5**:863-75.

22. Klappe K, Hummel I, Hoekstra D, Kok JW. Lipid dependence of ABC transporter localization and function. Chem Phys Lipids 2009;**161**:57-64.

23. Shen Q, Lin Y, Handa T, Doi M, Sugie M, Wakayama K, et al. Modulation of intestinal P-glycoprotein function by polyethylene glycols and their derivatives by in vitro transport and in situ absorption studies. Int J Pharm 2006;**313**:49-56.

24. Shen Q, Li W, Lin Y, Katsumi H, Okada N, Sakane T, et al. Modulating effect of polyethylene glycol on the intestinal transport and absorption of prednisolone, methylprednisolone and quinidine in rats by in-vitro and in-situ absorption studies. J Pharm Pharmacol 2008;**60**:1633-41.

25. Wang J, Qu H, Jin L, Zeng W, Qin L, Zhang F, et al. Pegylated phosphotidylethanolamine inhibiting P-glycoprotein expression and enhancing retention of doxorubicin in MCF7/ADR cells. J Pharm Sci 2011;**100**:2267-77.

26. Kang DI, Kang HK, Gwak HS, Han HK, Lim SJ. Liposome composition is important for retention of liposomal rhodamine in P-glycoprotein-overexpressing cancer cells. Drug Deliv 2009;**16**:261-67.

27. Li M, Si L, Pan H, Rabba AK, Yan F, Qiu J, et al. Excipients enhance intestinal absorption of gancyclovir by P-gp inhibition: assessed *in vitro* by everted gut sac and *in situ* by improbe intestinal perfusion. Int J Pharm 2011;**403**:37-45.

28. Zabaleta V, Ponchel G, Salman H, Agüeros M, Vauthier C, Irache JM. Oral administration of paclitaxel with pegylated poly(anhydride) nanoparticles: Permeability and pharmacokinetic study. Eur J Pharm Biopharm 2012;**81**:514-23.
29. Omote H, Figler RA, Polar MK, Al-Shawi MK. Improved energy coupling of human P-glycoprotein by the glycine 185 to valine mutation. Biochemistry 2004;**43**:3917-28.

Figure legends

Figure 1. Dose- and time-dependence of intracellular accumulation of liposomal doxorubicin formulations in drug-sensitive and drug-resistant cells

MCF7 and Pgp+ MCF7-dx cells were incubated with doxorubicin (dox), or liposomal doxorubicin formulations: anionic liposomes (A), neutral liposomes (N), cationic liposomes (C), PEGylated anionic liposomes (AP), PEGylated neutral liposomes (NP), PEGylated cationic liposomes (CP). **A-D**. Different concentrations (0-10 µmol/L) of doxorubicin and liposomal formulations were incubated for 24 h. **E-H**. Doxorubicin and liposomal formulations at 1 µmol/L were incubated for different time periods (0-24 h). The intracellular drug content was assessed fluorimetrically. The measurements were performed in triplicate and data are presented as mean ± SD (n = 3). For all panels: N or NP vs corresponding dox: * $p < 0.05$. Panels **B** and **D** (at each concentration): N vs corresponding A/C and NP vs corresponding AP/CP: $p < 0.05$; panels **E** and **G** (at time points 3-24 h) and panels **F** and **H** (at time points 1-24 h): N vs corresponding A/C and NP vs corresponding AP/CP: $p < 0.05$ (not reported).

Figure 2. Doxorubicin uptake and efflux of different liposomal doxorubicin formulations in drug-resistant cells

A-B. Pgp+ MCF7-dx cells were incubated at 37°C with 1 µmol/L doxorubicin (dox) or liposomal doxorubicin formulations: anionic liposomes (A), neutral liposomes (N), cationic liposomes (C), PEGylated anionic liposomes (AP), PEGylated neutral liposomes (NP), PEGylated cationic liposomes (CP). At fixed time points (0-20 min), cells were checked for the intracellular doxorubicin content. Measurements were performed in triplicate and data are presented as mean ± SD (n = 3). N or NP vs dox: * $p < 0.05$. At time points 5-20 min: N vs corresponding A/C and NP vs corresponding AP/CP: $p < 0.05$ (not reported). **C**. The uptake

benefit was calculated as reported under Methods. N or NP vs dox: * $p < 0.02$. N or NP vs the other liposomal formulations:° $p < 0.02$. **D-E.** Pgp+ MCF7-dx cells were incubated for 10 min with 1 µmol/L doxorubicin or liposomal doxorubicin formulations, as reported in panels **A-B**, then were washed five times and rinsed with 1 mL PBS. The extracellular amount of doxorubicin was measured fluorimetrically in triplicate immediately after washing (time 0) and at fixed time points up to 20 min. Data are presented as mean ± SD (n = 3). N or NP vs dox: * $p < 0.05$. At time points 5-20 min: N vs corresponding A/C and NP vs corresponding AP/CP: $p < 0.05$ (not reported). **F**. The efflux benefit was calculated as reported under Methods. N, NP or AP vs dox: * $p < 0.02$. N or NP vs the other liposomal formulations: ° $p < 0.05$. **G-H.** Pgp+ MCF7-dx cells were incubated for 20 min with increasing concentrations (0-100 µmol/L) of doxorubicin or liposomal doxorubicin formulations, then cells washed and tested for the intracellular drugs content. The procedure was repeated on a second series of dishes, incubated in the same experimental conditions and analyzed after 10 minutes further. Measurements (n = 3) were done in duplicate and data (mean ± SD) are presented as the rate of doxorubicin efflux (dc/dt) plotted versus the initial concentration of the drug. Vmax (nmol/min/mg proteins) and Km (nmol/mg proteins) were calculated with the Enzfitter software.

Figure 3. Effects of liposomal doxorubicin formulations on the ATPase activity of Pgp

Pgp+ MCF7-dx cells were lysed and the Pgp-rich membrane vesicles were isolated. **A-B.** Samples were incubated 30 min at 37°C with different concentrations (0-20 µmol/L) of verapamil, in the absence (ctrl) or presence of 1 µmol/L doxorubicin (dox) or liposomal doxorubicin formulations: anionic liposomes (A), neutral liposomes (N), cationic liposomes (C), PEGylated anionic liposomes (AP), PEGylated neutral liposomes (NP), PEGylated cationic liposomes (CP), to measure the maximal ATPase activity. **C-D.** Samples were

incubated for 30 min at 37°C with different concentrations (0-50 µmol/L) of doxorubicin or liposomal doxorubicin formulations, to measure the basal ATPase activity. Experiments were performed in triplicate and data are presented as mean ± SD (n = 3). For all panels: vs respective "0" concentration: * $p < 0.01$. Panel **A**: N vs corresponding A/C: $p < 0.05$ for 10-20 µmol/L; panel **B**: NP vs corresponding AP/CP: $p < 0.05$ for 5-20 µmol/L; panel **C**: N vs corresponding A/C: $p < 0.05$ for 1-50 µmol/; panel **D**: NP vs corresponding AP/CP: $p < 0.05$ for 0.1-50 µmol/L (not reported).

Figure 4. Effects of DSPE-PEG on Pgp ATPase activity and doxorubicin efflux

Pgp+ MCF7-dx cells were lysed and the Pgp-rich membrane vesicles were isolated. **A.** Samples were incubated for 30 min at 37°C with different concentrations (0-20 µmol/L) of verapamil, in the absence (ctrl) or presence of 1 µmol/L doxorubicin (dox), polyethylene-glycole (PEG), PEGylated distearoyl-phosphatidylethanolammine (DSPE-PEG), or DSPE-PEG and doxorubicin, to measure the maximal ATPase activity. **B.** Samples were incubated for 30 min at 37°C with different concentrations (0-50 µmol/L) of doxorubicin, PEG, DSPE-PEG, or DSPE-PEG and doxorubicin, to measure the basal ATPase activity. Experiments were performed in triplicate and data are presented as mean ± SD (n = 3). For both panels: DSPE-PEG or DSPE-PEG + dox vs respective "0" concentration: * $p < 0.005$. At each concentration: DSPE-PEG + dox vs dox: $p < 0.001$; PEG vs dox: $p < 0.002$; DSPE-PEG or DSPE-PEG + dox vs PEG: $p < 0.01$ (not reported). **C.** Pgp+ MCF7-dx cells were incubated for 20 min with increasing concentrations (0-100 µmol/L) of doxorubicin, or DSPE-PEG and doxorubicin, then washed and tested for the intracellular drugs content. The procedure was repeated on a second series of dishes, incubated in the same experimental conditions and analyzed after 10 minutes further. Measurements (n = 3) were performed in duplicate and data (mean ± SD) are presented as the rate of doxorubicin efflux (dc/dt) plotted versus the initial

concentration of the drug. Vmax (nmol/min/mg proteins) and Km (nmol/mg proteins) were calculated with the Enzfitter software.

Figure 5. Effect of DSPE-PEG on verapamil and colchicine binding to Pgp

The binding assay of [^{3}H]-verapamil (panel **A**) and [^{3}H]-colchicine (panel **B**), in the presence of increasing concentrations of cold verapamil or colchicine, doxorubicin (dox), PEGylated distearoyl-phosphatidylethanolammine (DSPE-PEG) or DSPE-PEG and doxorubicin, was performed on Pgp-rich membrane vesicles, isolated from Pgp+ MCF7-dx cells. Experiments were performed in quadruplicate and data are presented as mean ± SD (n = 3).

Figure 6. Effects of the G185V mutation on doxorubicin content and modulation of Pgp activity by DSPE-PEG

A. MCF7 cells, MCF7-dx cells, transfected with the pCDNA3 vector containing wild-type (Pgp wt) or mutated (Pgp G185V) *mdr1* sequence, were checked for the expression of Pgp/ABCB1 by Western blotting. The expression of the housekeeping protein actin was measured as equal loading control. The results shown here are representative of two similar experiments. **B.** The cell populations of panel **A** were incubated for 3 h with 5 µmol/L doxorubicin (dox), in the absence or presence of PEGylated distearoyl-phosphatidylethanolammine (DSPE-PEG); then the doxorubicin accumulation was detected fluorimetrically in duplicate. Data are presented as mean ± SD (n = 3). Vs corresponding condition in MCF7: * $p < 0.005$; DSPE-PEG + dox vs dox: ° $p < 0.001$. **C-D.** The binding assay of [^{3}H]-verapamil (panel **C**) and [^{3}H]-colchicine (panel **D**), in the presence of increasing concentrations of cold verapamil or colchicine, DSPE-PEG, or DSPE-PEG and doxorubicin, was performed on Pgp-rich membrane vesicles, isolated from G185V Pgp+ MCF7-dx cells. Experiments were performed in quadruplicate and data are presented as mean ± SD (n = 3).

E-F. G185V Pgp+ MCF7-dx cells were lysed and the Pgp-rich membrane vesicles were isolated. Panel **E**: samples were incubated for 30 min at 37°C with different concentrations (0-20 µmol/L) of verapamil, in the absence (ctrl) or presence of 1 µmol/L doxorubicin (dox), DSPE-PEG, DSPE-PEG and doxorubicin, PEGylated neutral liposomal doxorubicin (NP), to measure the maximal ATPase activity. Panel **F**: samples were incubated for 30 min at 37°C with different concentrations (0-50 µmol/L) of doxorubicin, DSPE-PEG, DSPE-PEG and doxorubicin, NP, to measure the basal ATPase activity. Experiments were performed in triplicate and data are presented as mean ± SD (n = 3).

Table 1. Liposomes composition and zeta potential (ζ)

Formulation	Lipid composition of liposomes	Lipid molar ratio	ζ (mV)
Neutral liposomes	DPPC*	-	-3,1
PEGylated neutral liposomes	DPPC/DSPE-PEG† 2000	1: 0.083	-10,9
Neutral liposomes	DPPC/chol‡	1: 0.66	-14
PEGylated neutral liposomes	DPPC/chol/DSPE-PEG 2000	1: 0.66: 0.083	-11,8
Anionic liposomes	DPPC/DPPG§	1 : 1	-40,1
PEGylated Anionic liposomes	DPPC/DPPG/DSPE-PEG 2000	1: 1: 0.16	-22,62
Anionic liposomes	DPPC/chol/DPPG	1 : 1.33 : 1	-63,1
PEGylated Anionic liposomes	DPPC/chol/DPPG/DSPE-PEG 2000	1: 1.33: 1: 0.16	-20,4
Cationic liposomes	DPPC/chol/DOTAP‖	1 : 1 : 1.33	29,84
PEGylated cationic liposomes	DPPC/chol/DOTAP/DSPE-PEG 2000	1 : 1 : 1.33 : 0.16	19,7

*DPPC: 1,2-dipalmitoyl-*sn*-glycero-3-phosphocholine; † DSPE-PEG: 1,2-diacyl-*sn*-glycero-3-phosphoethanolamine-N-[methoxy(polyethylene glycol)-2000; ‡ chol: cholesterol ; § DPPG: 1,2-dipalmitoyl-*sn*-glycero-3-phospho-rac-glycerol; ‖ DOTAP: 1,2-dioleoyloxy-3-trimethylammoniumpropanchloride

Table 2. Actual lipid and doxorubicin content of the liposome suspensions

Formulation	Actual total lipid content*	Actual DPPC content†	Actual loading‡	Encapsulation efficiency §
Neutral liposomes (no cholesterol?)	8.80	8.80	1.34 ± 0.16	89.56 ± 10.34
PEGylated neutral liposomes (no cholesterol?)	11.58	8.80	1.35 ± 0.09	89.89 ± 6.20
Neutral liposomes	11.90	8.80	1.34 ± 0.12	89.11 ± 7.69
PEGylated neutral liposomes	14.68	8.80	1.35 ± 0.15	90.22 ± 9.68
Anionic liposomes (no cholesterol?)	8.90	4.40	1.37 ± 0.08	91.22 ± 5.34
PEGylated Anionic liposomes (no cholesterol?)	11.68	4.40	1.37 ± 0.06	91.44 ± 4.33
Anionic liposomes	11.96	4.40	1.39 ± 0.09	92.44 ± 6.32
PEGylated Anionic liposomes	14.74	4.40	1.38 ± 0.10	92.33 ± 6.91
Cationic liposomes	11.70	4.40	1.25 ± 0.11	83.22 ± 7.62
PEGylated cationic liposomes	14.50	4.40	1.21 ± 0.10	80.56 ± 6.59

* expressed as mg of total lipid *per* ml of liposome suspension

† expressed as mg of total lipid *per* ml of liposome suspension

‡ doxorubicin concentration within each liposome formulation after gel filtration, expressed as mmol/L; results are expressed as mean ± SD (n = 6)

§ ratio (percentage of actual doxorubicin encapsulated in each formulation/ percentage of expected doxorubicin encapsulated in each formulation); results are expressed as mean percentages ± SD (n = 6)

Supplementary materials

Extended Methods

Chemicals. 1,2-dioleoyloxy-3-trimethylammoniumpropanchloride (DOTAP), 1,2-dipalmitoyl-*sn*-glycero-3-phospho-rac-glycerol sodium salt (DPPG-Na), 1,2-dipalmitoyl-*sn*-glycero-3-phosphocholine (DPPC) and 1,2-diacyl-*sn*-glycero-3-phosphoethanolamine-N-[methoxy(polyethylene glycol)-2000] (DSPE-PEG2000) were kindly offered by Lipoid GmbH (Cam, Switzerland). Cholesterol (chol), Sephadex G-50, ammonium sulfate, 4-(2-hydroxyethyl)piperazine-1-ethanesulfonic acid, N-(2-hydroxyethyl)piperazine-N′-(2-ethanesulfonic acid) (HEPES), ammonium thiocyanate, iron(III) chloride anhydrous, were obtained from Sigma Chemical Co. (St. Louis Mo, USA). Methanol, chloroform and analytical grade diethyl ether were purchased from Carlo Erba (Milan, Italy). High pure water was prepared by using Millipore (Molsheim, France) Milli Q plus filtration system. Foetal bovine serum (FBS) and culture medium were supplied by Invitrogen Life Technologies (Carlsbad, CA); plasticware for cell cultures was from Falcon (Becton Dickinson, Franklin Lakes, NJ). Electrophoresis reagents were obtained from Bio-Rad Laboratories (Hercules, CA); the protein content of cell monolayers and lysates was assessed with the BCA kit from Sigma Chemical Co. (St. Louis, MO). [^{3}H]-verapamil, [^{3}H]-colchicine and [^{3}H]-vinblastine were from PerkinElmer (Waltham, MA). When not otherwise specified, all the other reagents were purchased from Sigma Chemical Co.

Liposome preparation. Liposomes composed of DPPC, DPPC/chol (1:0.66 molar ratio), DPPC/DSPE-PEG 2000 (1:0.083 molar ratio), DPPC/chol/DSPE-PEG 2000 (1:0.66:0.083 molar ratio), DPPC/DPPG (1:1 molar ratio), DPPC/chol/DPPG (1:1.33:1 molar ratio), DPPC/DPPG/DSPE-PEG 2000 (1:1:0.16 molar ratio), DPPC/chol/DPPG/DSPE-PEG 2000 (1:1.33:1:0.16 molar ratio) were prepared by hydration of a thin lipid film. Briefly, the lipid mixture was dissolved in chloroform/methanol (2:1 v/v). This organic solution was added to a 50 mL round-bottom flask, and the solvent was removed under reduced pressure by a rotary evaporator under

nitrogen atmosphere. The resulting lipid film was dispersed in 1 mL ammonium sulfate buffer 250 mmol/L in presence of glass beads (Sigma) and incubated at 50°C for 2 h. The resulting suspension was then repeatedly extruded under nitrogen through polycarbonate membrane (Nucleopore Track Membrane 25 mm, Whatman, Brentford, UK) with 0.4 µm, 0.2 µm, and 0.1 µm pore size at 50°C using a thermobarrel extruder system (Northern Lipids Inc., Vancouver, BC, Canada). Liposome external medium was then replaced with Hepes buffer 250 mmol/L pH 7.4, by means of 3 cycles, each at 80,000 rpm for 40 min at 4°C of ultracentrifugation (Optima Max E, Beckman Coulter, USA). Liposomes composed of either DPPC/Chol/DOTAP (1:1:1.33 molar ratio) or DPPC/Chol/DOTAP/DSPE-PEG 2000 (1:1:1.33:0.16 molar ratio) were dissolved in a mixture chloroform/methanol (2:1 v/v). This solution was added to a 50 mL round-bottom flask, and the solvent was removed under reduced pressure by a rotary evaporator under nitrogen atmosphere. The resulting lipid film was dissolved in 3 mL diethyl ether and the solution was emulsified by sonication for 30 min in a bath-type sonicator (Branson 3510, Danbury, USA), with 1 mL of ammonium sulfate buffer 250 mmol/L in presence of glass beads (Sigma). The resulting emulsion was then placed on the rotary evaporator (Laborota 4010 digital, Heidolph, Schwabach, Germany) and the organic solvent was removed under reduced pressure at 30°C in nitrogen atmosphere. When viscous gel was obtained, the vacuum was broken and the gel was vortexed for about 1 min. The dispersion was placed in a rotary evaporator under vacuum for about 15 min and then incubated at 50°C for 30 min. The resulting suspension was then repeatedly extruded using a thermobarrel extruder system as previously described. The liposome suspension was purified through Sephadex G-50 column and eluted in an aqueous solution containing 250 mmol/L Hepes buffer at pH 7.4.

All liposome preparations were stored at 4°C. Each formulation was prepared in triplicate.

For doxorubicin loading, 1.5 mmol/L doxorubicin in sterile aqueous solution was added to each liposome preparation. The residual non-encapsulated drug was removed by gel filtration in a

Sephadex G-50 (Amersham Bioscience, Piscataway, NJ, USA) column. The liposomes were stored at a doxorubicin concentration of 0.5 mmol/L at 4°C and used in the subsequent experiments.

Liposome characterization. The mean diameter of the liposomes, before and after purification, was determined at 20°C by photon correlation spectroscopy (PCS) (N5, Beckman Coulter, Miami, USA). Each sample was diluted in deionizer/filtered (0.22 m pore size, polycarbonate filters, MF-Millipore, Microglass Heim, Italy) water and analyzed with detector at 90° angle. As measure of the particle size distribution, polydispersity index (P.I.) was used. For each batch, mean diameter and size distribution were the mean of three measurements. For each formulation, the mean diameter and P.I. were calculated as the mean of three different batches. The zeta-potential (ζ) of liposomes was determined by means of a Zetasizer Nano Z (Malvern, UK). For each batch, ζ was calculated as the mean of five measurements. For each formulation, ζ was calculated as the mean of three different batches.

To determine the phospholipid content of the liposome formulations, an aliquot of the liposome suspension was added to a two-phase system, consisting of an aqueous ammonium ferrithiocyanate solution (0.1 N) and chloroform. The concentration of PC and DSPE-PEG was obtained by a calibration curve calculated by lipid concentration versus absorbance at 485 nm into the organic layer.

The amount of encapsulated doxorubicin was quantified by diluting 50 μL of liposomal suspension in 0.5 ml of 1:1 v/v ethanol/HCl 0.3 N, sonicating the liposomes and measuring the fluorescence emitted by the drug with a LS-5 spectrofluorimeter (PerkinElmer). Excitation and emission wavelengths were 475 nm and 553 nm respectively.

Western blot analysis. Cells were rinsed with boiling 0.5 mL lysis buffer (10 mmol/L Tris, 100 mmol/L NaCl, 20 mmol/L KH_2PO_4, 30 mmol/L EDTA, 1 mmol/L EGTA, 250 mmol/L sucrose; pH 7.5). After sonication 1 mmol/L Na_3VO_4, 1 mmol/L NaF, 10 mmol/L dithiothreitol and the inhibitor

cocktail set III [100 mmol/L 4-(2-aminoethyl)benzenesulfonyl fluoride, 80 mmol/L aprotinin, 5 mmol/L bestatin, 1.5 mmol/L E-64, 2 mmol/L leupeptin, 1 mmol/L pepstatin; Calbiochem, San Diego, CA] were added and cell lysates were centrifuged at 13,000 x g for 15 min. 50 µg cell proteins were separated by SDS-PAGE and probed with anti-Pgp/ABCB1 (C219, Calbiochem), anti-MRP1/ABCC1 (Abcam, Cambridge, UK), anti-BCRP/ABCG2 (Santa Cruz Biotechnology, Santa Cruz, CA) and anti-actin antibody (Sigma Chemical Co.), used as control of equal loading.

Liposomes intracellular distribution. 5×10^5 cells were grown on sterile glass coverslips, labelled with the lysosomes specific probe Lysotracker Red (Invitrogen Life Technologies), then incubated for 10 min with with 1 µmol/L liposomes containing cholesterol-NBD (22-(N-(7-nitrobenz-2-oxa-1,3-diazol-4-yl)amino)-23,24-bisnor-5-cholen-3β-ol as fluorophore. At the end of the incubation period, cells were rinsed with PBS, fixed with 4% w/v paraformaldehyde for 15 min, washed three times with PBS and once with water, then the slides were mounted with 4 µL of Gel Mount Aqueous Mounting and examined. Image acquisition was performed with a Leica TCS SP2 AOBS confocal laser-scanning microscope (Leica Microsystems, Wetzlar, Germany) with a 60 × oil immersion objective and 10× ocular lens. For each experimental point, a minimum of five microscopic fields were examined.

Kinetic parameters of doxorubicin efflux. MCF7-dx cells were incubated for 20 min with increasing (0-100 µmol/L) concentrations of doxorubicin or liposomal doxorubicin formulations, then washed and analysed for the intracellular concentration of doxorubicin. A second series of dishes, after the incubation with doxorubicin or liposomal formulations under the same experimental conditions, were left for further 10 min at 37°C, then washed and tested for the intracellular drug content. The difference of doxorubicin concentration between the two series, expressed as nmol doxorubicin extruded/min/mg cell protein was plotted versus the initial drugs concentration. Values were fitted to Michaelis-Menten equation to calculate Vmax and Km, using the Enzfitter software (Biosoft Corporation, Cambridge, United Kingdom).

ATPase assay. The assay was performed on Pgp-rich membrane vesicles according to [1], with minor modifications. Cells were washed with Ringer's solution (148.7 mmol/L NaCl, 2.55 mmol/L K_2HPO_4, 0.45 mmol/L KH_2PO_4, 1.2 mmol/L $MgSO_4$; pH 7.4), lysed on crushed ice with lysis buffer (10 mmol/L Hepes/Tris, 5 mmol/L EDTA, 5 mmol/L EGTA, 2 mmol/L dithiothreitol; pH 7.4) supplemented with 2 mmol/L phenylmethylsulfonyl fluoride, 1 mmol/L aprotinin, 10 μg/mL pepstatin, 10 μg/mL leupeptin, and subjected to nitrogen cavitation at 1200 psi for 20 min. Samples were centrifuged at 300 x g for 10 min, diluted 1:4 in the pre-centrifugation buffer (10 mmol/L Tris/HCl, 25 mmol/L sucrose; pH 7.5), overlaid on a sucrose cushion (10 mmol/L Tris/HCl, 35% w/v sucrose, 1 mmol/L EDTA; pH 7.5) and centrifuged at 14,000 x g for 10 min. The interface was collected, diluted 1:5 in the centrifugation buffer (10 mmol/L Tris/HCl, 250 mmol/L sucrose; pH 7.5) and subjected to a third centrifugation at 100,000 x g for 45 min. The vesicles pellet was re-suspended in 0.5 mL centrifugation buffer and stored at -80°C until the use, after the quantification of the protein content. For basal ATPase assays, samples (containing 20 μg protein) were incubated for 30 min at 37°C with 50 μL of the reaction mix (25 mmol/L Tris/HCl, 3 mmol/L ATP, 50 mmol/L KCl, 2.5 mmol/L $MgSO_4$, 3 mmol/L dithiothreitol, 0.5 mmol/L EGTA, 2 mmol/L ouabain, 3 mmol/L NaN_3; pH 7.0), in the absence or presence of increasing concentrations (0-50 μmol/L) of doxorubicin or liposomal doxorubicin formulations. For the verapamil-stimulated ATPase activity, taken as index of the maximal Pgp activity, samples were incubated with 1 μmol/L doxorubicin or liposomal doxorubicin formulations, in the presence of increasing concentrations (0-20 μmol/L) of verapamil. In each set of experiments, a blank containing 0.5 mmol/L Na_3VO_4 was included. The reaction was stopped by adding 0.2 mL ice-cold stopping buffer (0.2% w/v ammonium molybdate, 1.3% v/v H_2SO_4, 0.9% w/v SDS, 2.3% w/v trichloroacetic acid, 1% w/v ascorbic acid). After a 30-min incubation at room temperature, the absorbance of the phosphate hydrolyzed from ATP was measured at 620 nm, using a Packard EL340 microplate reader (Bio-Tek Instruments, Winooski, MA). The absorbance was converted into μmol hydrolyzed phosphate/min/mg prot, according to the titration curve previously prepared.

Verapamil and colchicine binding. Pgp-rich membrane vesicles containing 10 μg proteins were incubated in MultiScreen 96-wells plate 0.22 μm pore-size (Millipore, Billerica, MA) for 30 min at room temperature with 1.2 nmol/L [^{3}H]-verapamil, 1 nmol/L [^{3}H]-colchicine or 1 nmol/L [^{3}H]-vinblastine, in 0.1 mL of binding buffer (50 mmol/L Tris/HCl, pH 7.4); in the absence or presence of different concentrations of doxorubicin, PEGylated distearoyl-phosphatidylethanolammine (DSPE-PEG) or cold ligands, as indicated in the Results section. The reaction was stopped by adding 0.25 mL ice-cold wash buffer (20 mmol/L Tris/HCl, 50 mmol/L $MgSO_4$; pH 7.4). Samples were rapidly filtered and the amount of radioactivity entrapped on filters was detected by liquid scintillation count. The non specific binding was quantified by incubating samples with 1 mmol/L rhodamine 123 and was subtracted from the total binding. The radioactivity was converted into fmol radioligand bound/mg protein, according to the respective titration curves. For each experimental point the results were expressed as fraction of the maximal binding capacity (Bmax).

References

1. Litman T, Zeuthen T, Svovgaard T, Stein WD. Competitive, non-competitive and cooperative interactions between substrates of P-glycoprotein as measured by its ATPase activity. Biochim Biophys Acta 1997; **1361:**169-76.

Supplementary Figures

Supplementary Figure 1

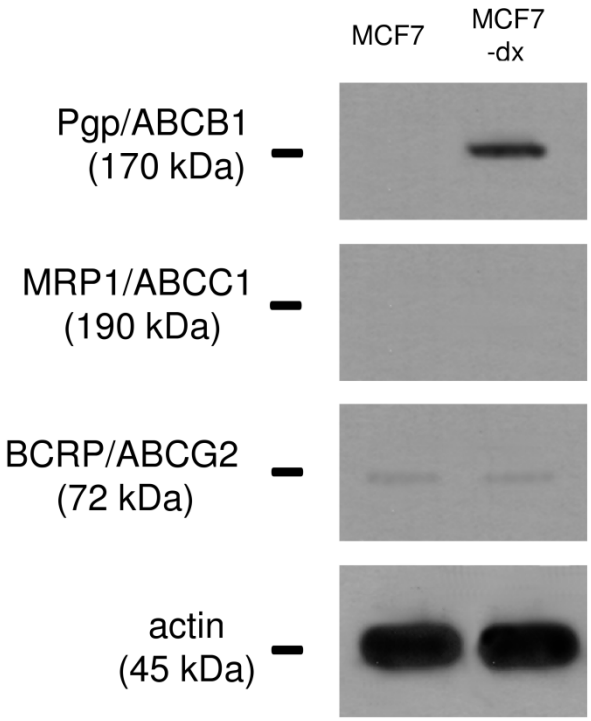

Supplementary Figure 1. Expression of ABC transporters expression in MCF-7 and MCF7-dx cells.

MCF7 cells and Pgp+ MCF7-dx cells, transfected with pCDNA3 vector containing the wild-type *mdr1* sequence, were checked for the expression of Pgp/ABCB1, MRP1/ABCC1 and BCRP/ABCG2 by Western blotting. The expression of the housekeeping protein actin was measured as equal loading control. The results shown here are representative of two similar experiments.

Supplementary Figure 2

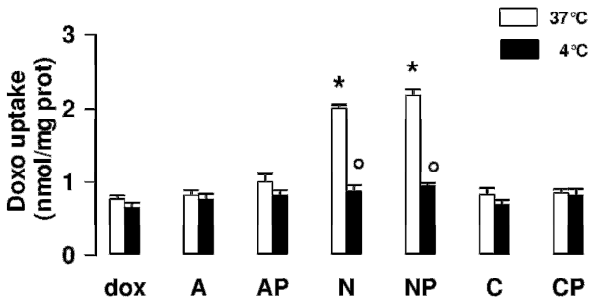

Supplementary Figure 2. Effects of temperature on the uptake of liposomal doxorubicin formulations.

Pgp+ MCF7-dx cells were incubated at 37°C or 4°C with 1 μmol/L doxorubicin (dox) or liposomal formulations: anionic liposomes (A), neutral liposomes (N), cationic liposomes (C), PEGylated anionic liposomes (AP), PEGylated neutral liposomes (NP), PEGylated cationic liposomes (CP). After 20 min, the intracellular doxorubicin content was measured in duplicate fluorimetrically. Data are presented as mean $\pm$ SD (n = 3). N or NP vs corresponding dox: * $p < 0.001$; N or NP at 4°C vs 37°C: :° $p < 0.001$.

Supplementary Figure 3

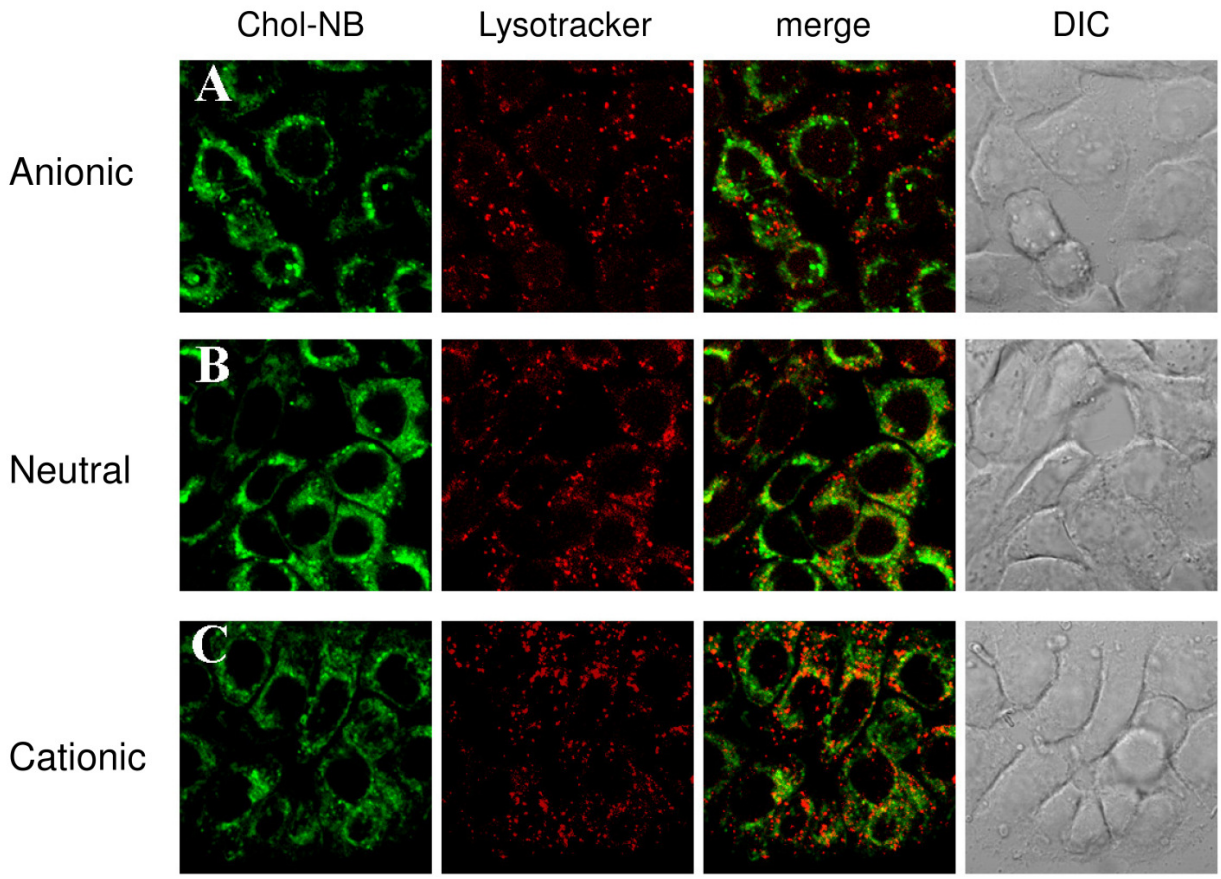

Supplementary Figure 3. Intracellular distribution of non PEGylated liposomes.

Pgp+ MCF7-dx cells were labeled with the lysosome-specific probe Lysotracker Red (50 nmol/L for 2 h), then incubated for 10 min at 37°C with 1 μmol/L of anionic (panels **A**), neutral (panels **B**) or cationic (panels **C**) liposomes, containing the fluorescent lipid chol-NBD (22-(N-(7-nitrobenz-2-oxa-1,3-diazol-4-yl)amino)-23,24-bisnor-5-cholen-3β-ol) (chol-NB). Cells were then washed, fixed and analyzed by confocal microscope. The samples were analyzed by Nomarski differential interference contrast optics (DIC). Magnification: 60 × objective (1.4 numerical aperture); 10 × ocular lens.The images are representative of two experiments with similar results.

Supplementary Figure 4

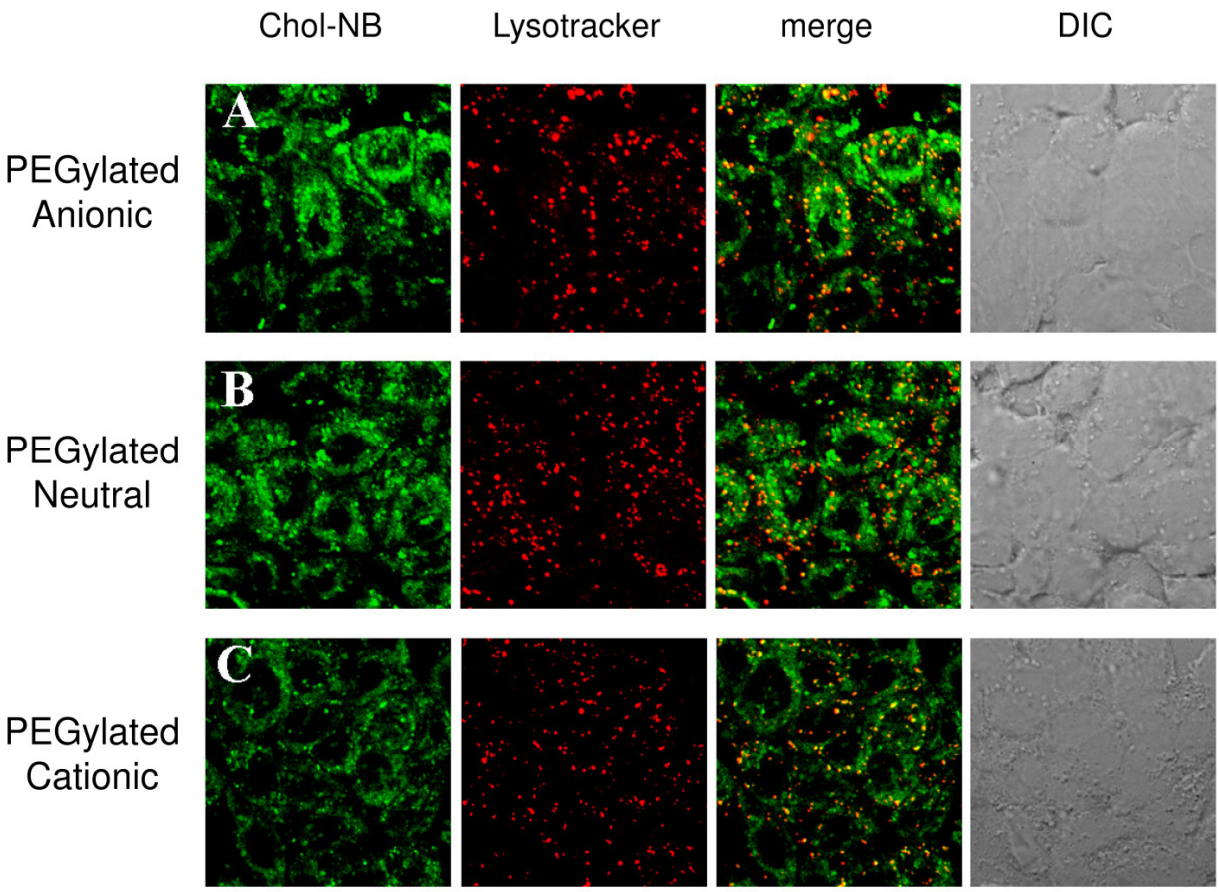

Supplementary Figure 4. Intracellular distribution of PEGylated liposomes.

Pgp+ MCF7-dx cells were labeled with the lysosomes specific probe Lysotracker Red (50 nmol/L for 2 h), then incubated for 10 min at 37°C with 1 μmol/L PEGylated anionic (panels **A**), PEGylated neutral (panels **B**), PEGylated cationic (panels **C**) liposomes, containing the fluorescent lipid chol-NBD (22-(N-(7-nitrobenz-2-oxa-1,3-diazol-4-yl)amino)-23,24-bisnor-5-cholen-3β-ol) (chol-NB). Cells were then washed, fixed and analyzed by confocal microscope. The samples were analyzed by Nomarski differential interference contrast optics (DIC). Magnification: 60 × objective (1.4 numerical aperture); 10 × ocular lens.The images are representative of two experiments with similar results.

Supplementary Figure 5

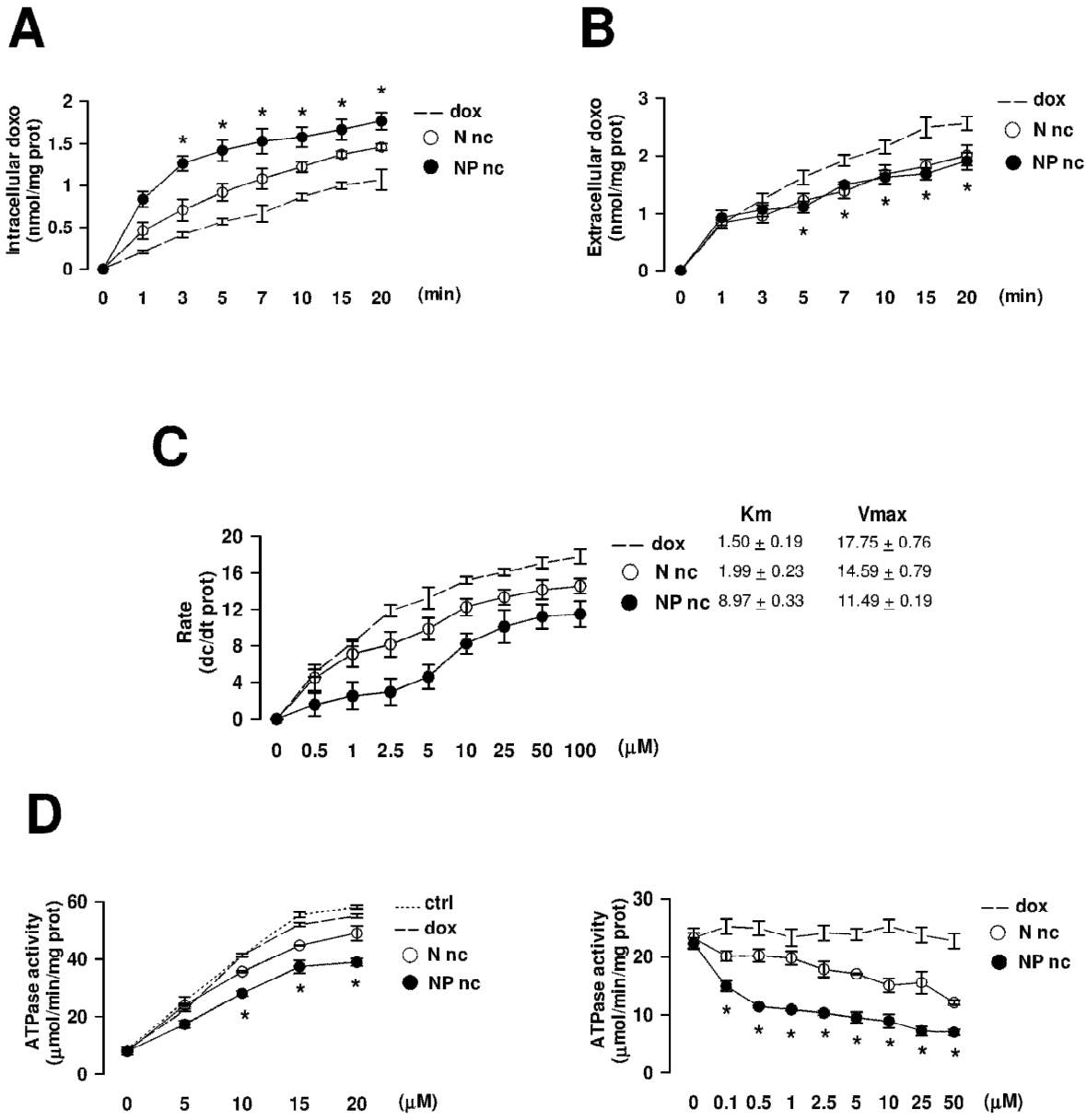

Supplementary Figure 5. Effects of cholesterol-free liposomes on doxorubicin uptake, doxorubicin efflux and Pgp activity.

A. Doxorubicin uptake. Pgp+ MCF7-dx cells were incubated at 37°C with 1 μmol/L doxorubicin (dox), cholesterol-free neutral liposomal doxorubicin (N nc) or cholesterol-free PEGylated neutral

liposomal doxorubicin (NP nc). At fixed time points (0-20 min), cells were checked for the intracellular doxorubicin content. Measurements were performed in triplicate and data are presented as mean $\pm$ SD (n = 3). NP nc or N nc vs dox: * $p < 0.005$; NP nc vs N nc: $p < 0.05$ (not reported). Not significant difference was observed at each time point vs N or NP containing cholesterol (see Fig. 2A). **B.** Doxorubicin efflux. Pgp+ MCF7-dx cells were incubated for 10 min with 1 μmol/L doxorubicin (dox), cholesterol-free neutral liposomal doxorubicin (N nc) or cholesterol-free PEGylated neutral liposomal doxorubicin (NP nc). Then cells were washed five times and rinsed with 1 mL PBS; the extracellular amount of doxorubicin was measured fluorimetrically in triplicate immediately after washing (time 0) and at fixed time points up to 20 min. Data are presented as mean $\pm$ SD (n = 3). NP nc or N nc vs dox: * $p < 0.05$. No significance was observed at each time point vs N or NP containing cholesterol (see Fig. 2C). **C.** Kinetics of Pgp activity. Pgp+ MCF7-dx cells were incubated for 20 min with increasing concentrations (0-100 μmol/L) of doxorubicin (dox), cholesterol-free neutral liposomal doxorubicin (N nc) or cholesterol-free PEGylated neutral liposomal doxorubicin (NP nc). Then cells were washed and tested for the intracellular drug content. The procedure was repeated on a second series of dishes, incubated in the same experimental conditions and analysed after 10 minutes further. Measurements (n = 3) were done in duplicate and data (mean $\pm$ SD) are presented as the rate of efflux (dc/dt) plotted versus the initial concentration of the drugs. Vmax (nmol/min/mg protein) and Km (nmol/mg protein) were calculated with the Enzfitter software. No significant difference was observed for each concentration vs neutral or PEGylated neutral liposomal doxorubicin containing cholesterol (see Fig. 2E). **D.** Left panel: verapamil-stimulated Pgp ATPase activity. Pgp-rich membrane vesicles, isolated from Pgp+ MCF7-dx cells, were incubated for 30 min at 37°C with different concentrations (0-20 μmol/L) of verapamil, in the absence (ctrl) or presence of 1 μmol/L doxorubicin (dox), cholesterol-free neutral liposomal doxorubicin (N nc) or cholesterol-free PEGylated neutral liposomal doxorubicin (NP nc), to measure the maximal ATPase activity. Right panel: basal Pgp ATPase activity. Samples were incubated 30 min at 37°C with different concentrations (0-50

μmol/L) of doxorubicin (dox), cholesterol-free neutral liposomal doxorubicin (N nc) or cholesterol-free PEGylated neutral liposomal doxorubicin (NP nc), to measure the basal ATPase activity. Experiments were performed in triplicate and data are presented as mean $\pm$ SD (n = 3). Both panels: NP nc vs respective "0" concentration: * $p < 0.005$; NP nc vs N nc: $p < 0.05$ (not reported). Left panel: N nc or NP nc vs dox: $p < 0.05$ at 10-20 μmol/L; right panel: N nc or NP nc vs dox: $p < 0.05$ at 0.1-50 μmol/L (not reported). No significant difference observed for each experimental condition vs N or NP containing cholesterol (see Figure 3).

Figure 1

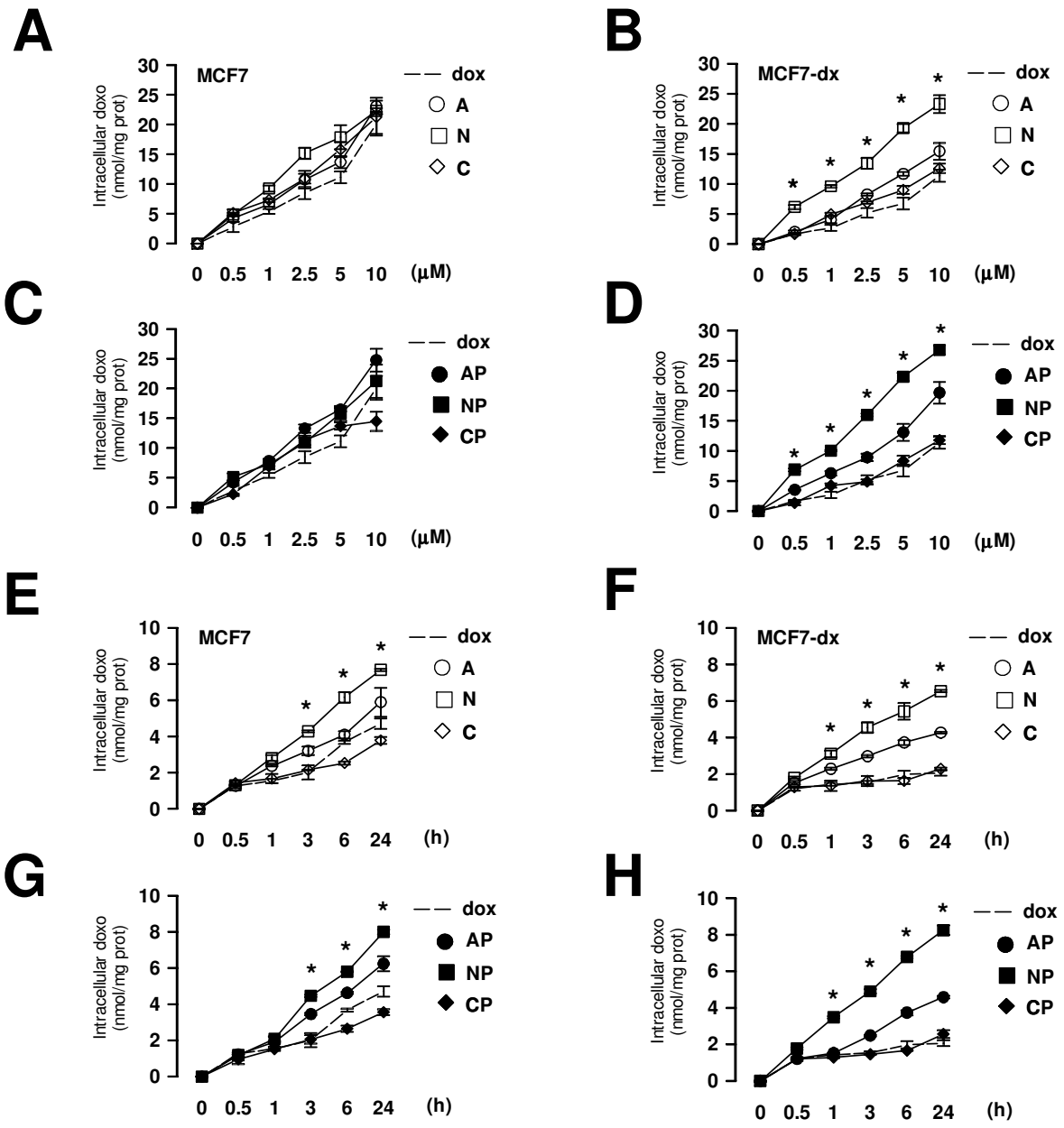
A
MCF7
dox
A
N
C
Intracellular doxo (nmol/mg prot)
0 0.5 1 2.5 5 10 (μM)
B
MCF7-dx
C
AP
NP
CP
D
E
0 0.5 1 3 6 24 (h)
F
G
H

Figure 2

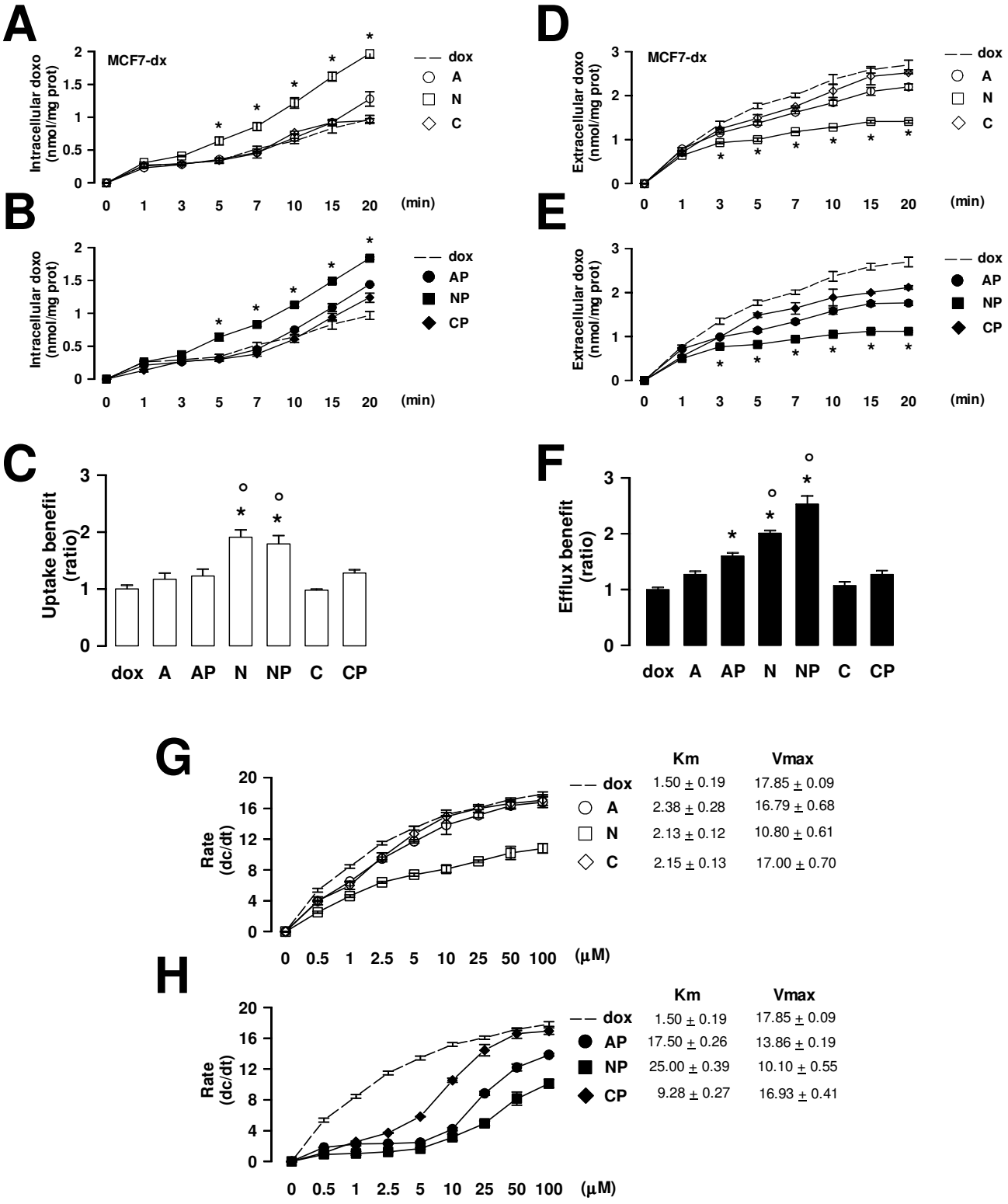
A
MCF7-dx
Intracellular doxo (nmol/mg prot)
dox
A
N
C
(min)
B
AP
NP
CP
D
Extracellular doxo (nmol/mg prot)
E
C
Uptake benefit (ratio)
dox A AP N NP C CP
F
Efflux benefit (ratio)
G
Rate (dc/dt)
(μM)
Km
Vmax
dox 1.50 ± 0.19 17.85 ± 0.09
A 2.38 ± 0.28 16.79 ± 0.68
N 2.13 ± 0.12 10.80 ± 0.61
C 2.15 ± 0.13 17.00 ± 0.70
H
AP 17.50 ± 0.26 13.86 ± 0.19
NP 25.00 ± 0.39 10.10 ± 0.55
CP 9.28 ± 0.27 16.93 ± 0.41

Figure 3

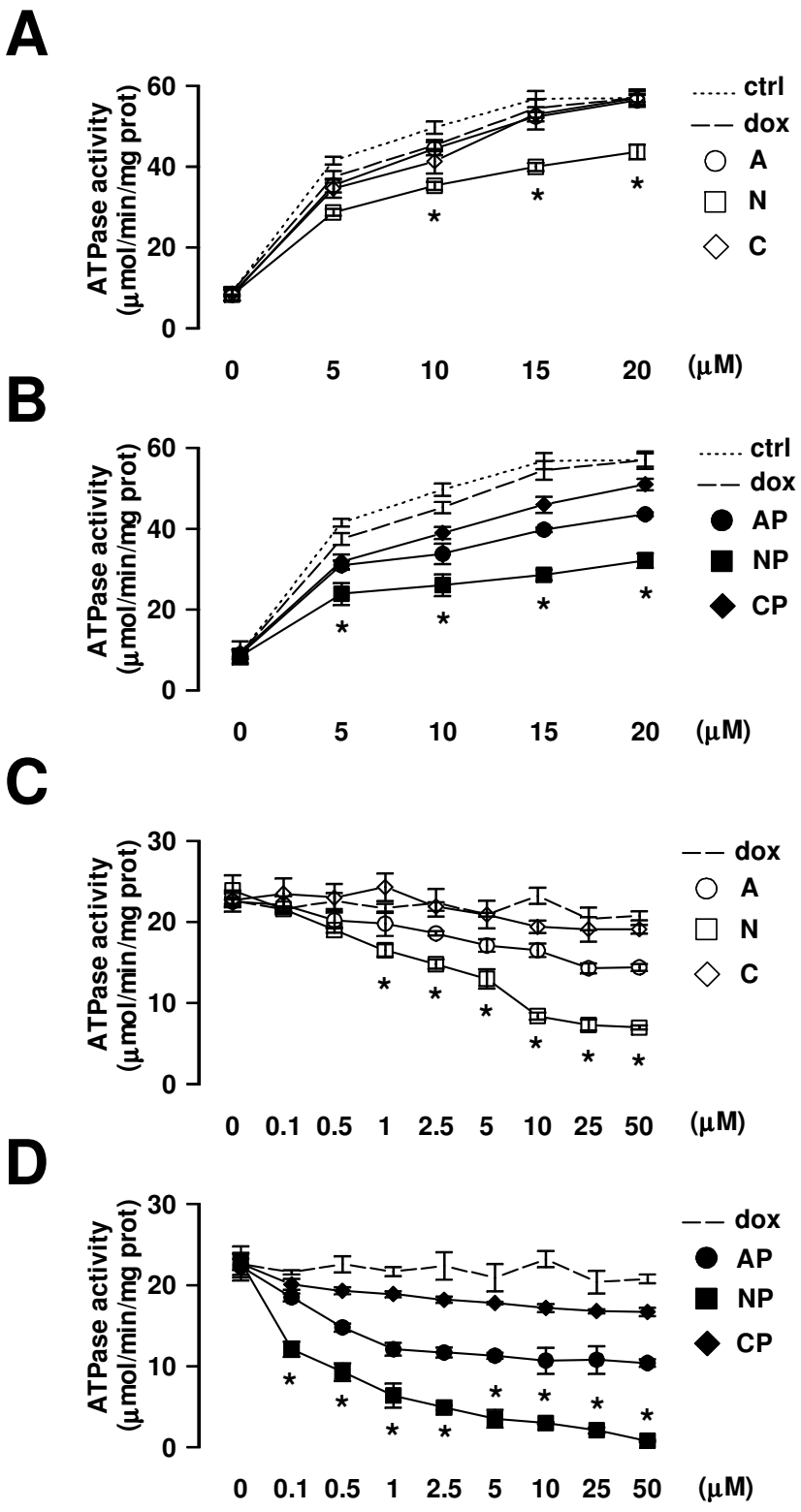
A
ATPase activity (µmol/min/mg prot)
60
40
20
0
ctrl
dox
A
N
C
0 5 10 15 20 (µM)
B
ATPase activity (µmol/min/mg prot)
60
40
20
0
ctrl
dox
AP
NP
CP
0 5 10 15 20 (µM)
C
ATPase activity (µmol/min/mg prot)
30
20
10
0
dox
A
N
C
0 0.1 0.5 1 2.5 5 10 25 50 (µM)
D
ATPase activity (µmol/min/mg prot)
30
20
10
0
dox
AP
NP
CP
0 0.1 0.5 1 2.5 5 10 25 50 (µM)

Figure 4

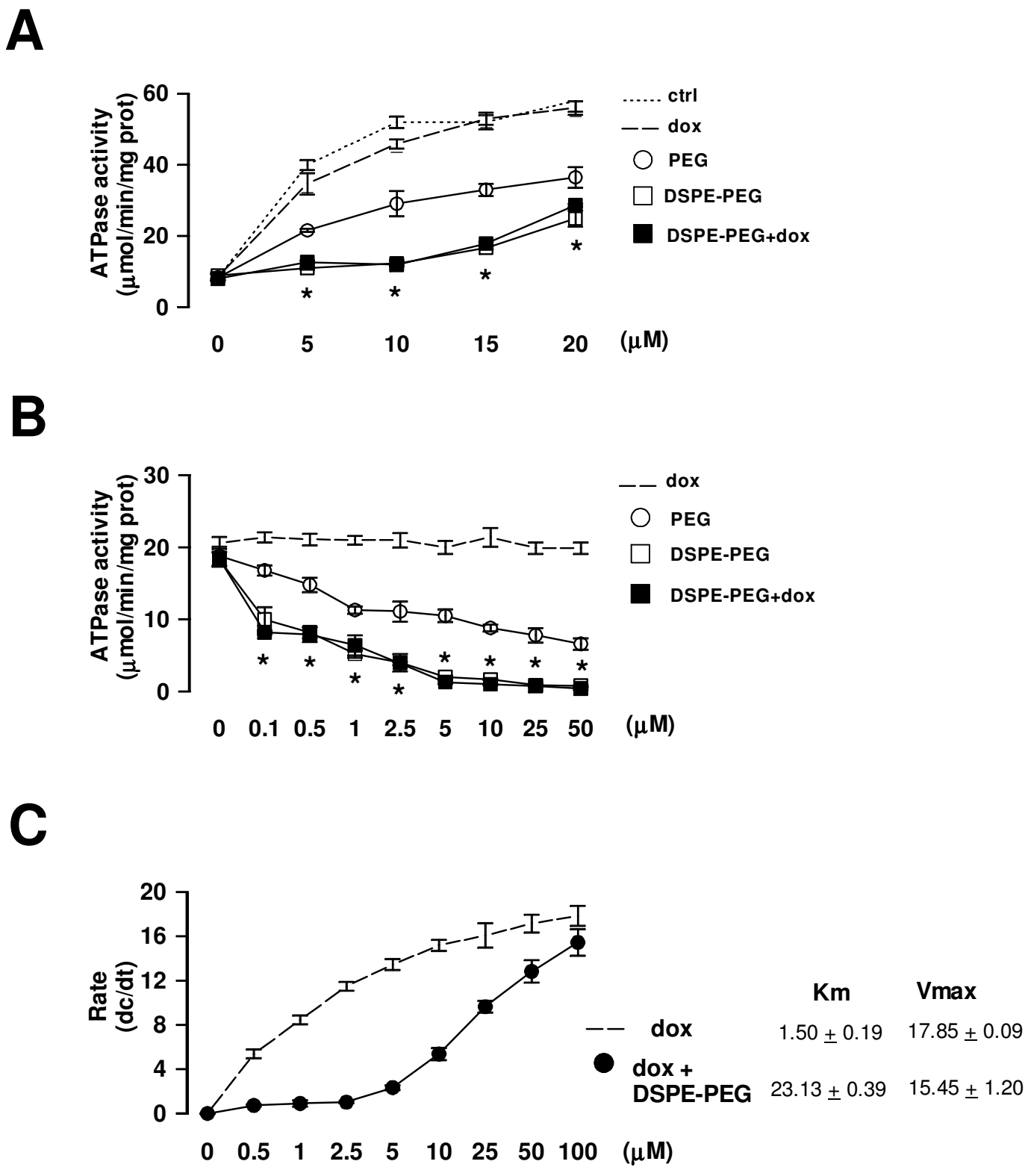
A
ATPase activity (μmol/min/mg prot)
60
40
20
0
ctrl
dox
PEG
DSPE-PEG
DSPE-PEG+dox
0
5
10
15
20
(μM)
B
ATPase activity (μmol/min/mg prot)
30
20
10
0
dox
PEG
DSPE-PEG
DSPE-PEG+dox
0
0.1
0.5
1
2.5
5
10
25
50
(μM)
C
Rate (dc/dt)
20
16
12
8
4
0
0
0.5
1
2.5
5
10
25
50
100
(μM)
dox
dox + DSPE-PEG
Km
Vmax
1.50 ± 0.19
17.85 ± 0.09
23.13 ± 0.39
15.45 ± 1.20

Figure 5

A

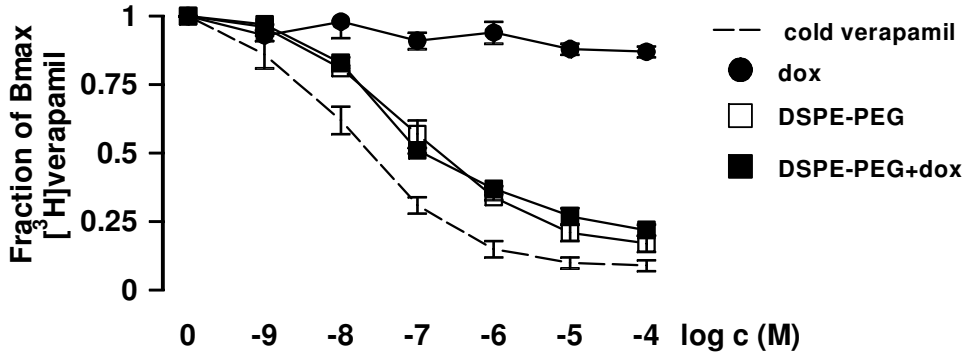
Fraction of Bmax
[3H]verapamil
1
0.75
0.5
0.25
0
0 -9 -8 -7 -6 -5 -4 log c (M)
cold verapamil
dox
DSPE-PEG
DSPE-PEG+dox

B

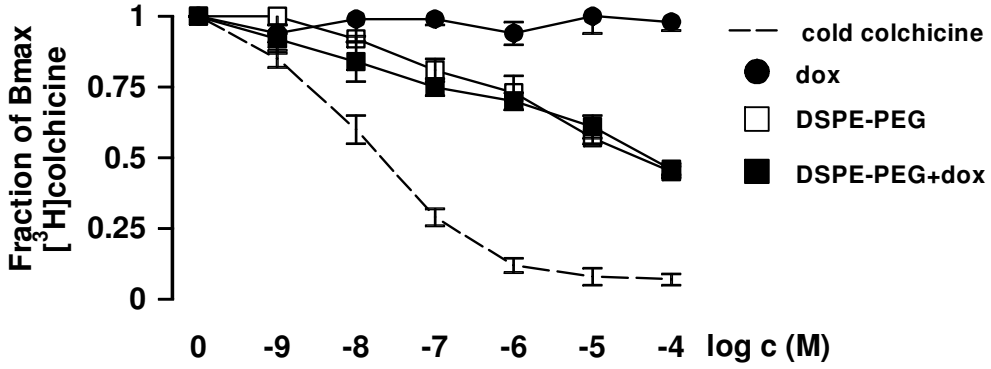
Fraction of Bmax
[3H]colchicine
1
0.75
0.5
0.25
0
0 -9 -8 -7 -6 -5 -4 log c (M)
cold colchicine
dox
DSPE-PEG
DSPE-PEG+dox

Figure 6

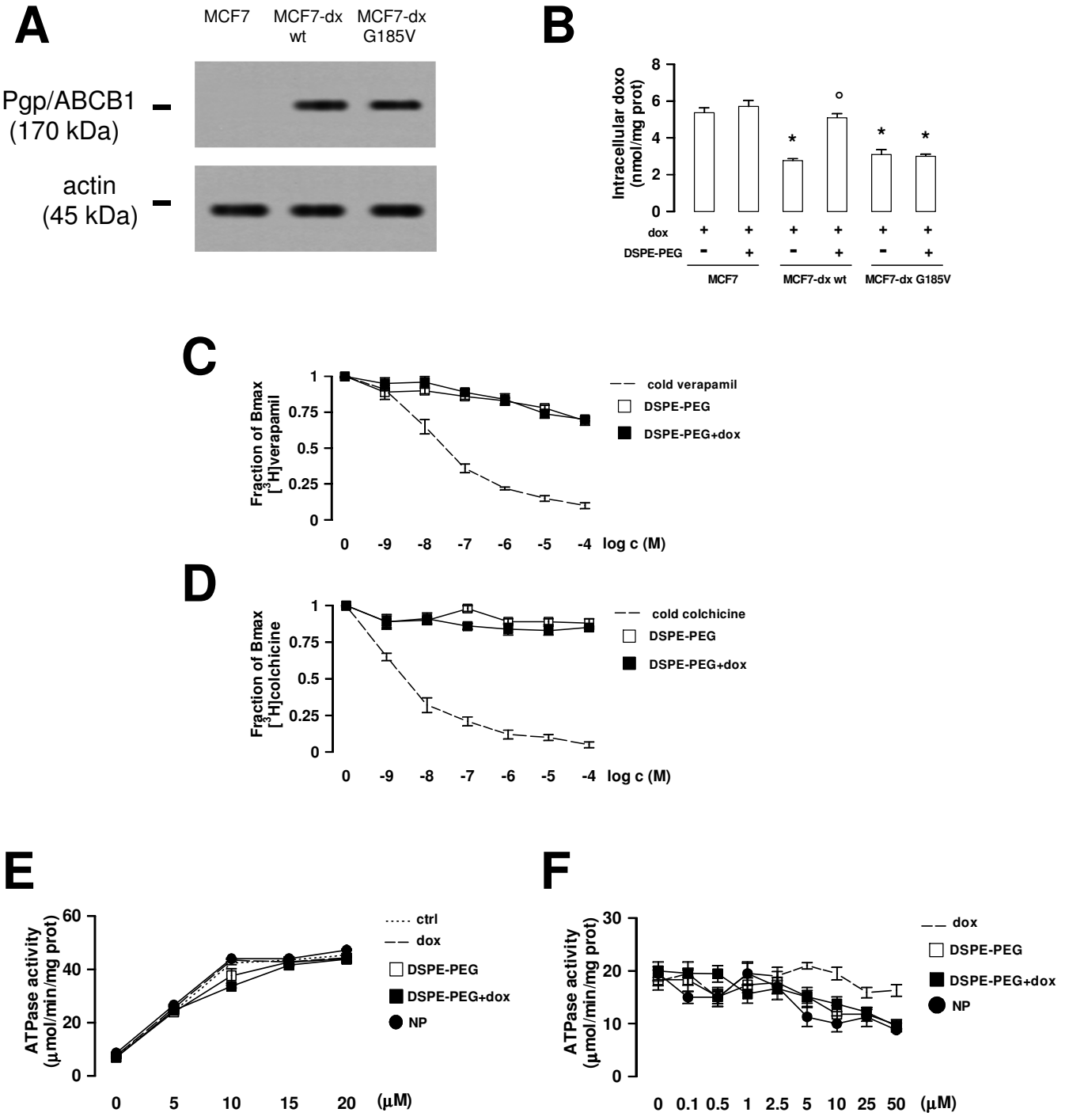
A
MCF7
MCF7-dx wt
MCF7-dx G185V
Pgp/ABCB1 (170 kDa)
actin (45 kDa)
B
Intracellular doxo (nmol/mg prot)
dox
DSPE-PEG
MCF7
MCF7-dx wt
MCF7-dx G185V
C
Fraction of Bmax [3H]verapamil
cold verapamil
DSPE-PEG
DSPE-PEG+dox
log c (M)
D
Fraction of Bmax [3H]colchicine
cold colchicine
DSPE-PEG
DSPE-PEG+dox
log c (M)
E
ATPase activity (µmol/min/mg prot)
ctrl
dox
DSPE-PEG
DSPE-PEG+dox
NP
(µM)
F
ATPase activity (µmol/min/mg prot)
dox
DSPE-PEG
DSPE-PEG+dox
NP
(µM)

Supplementary Figure 1

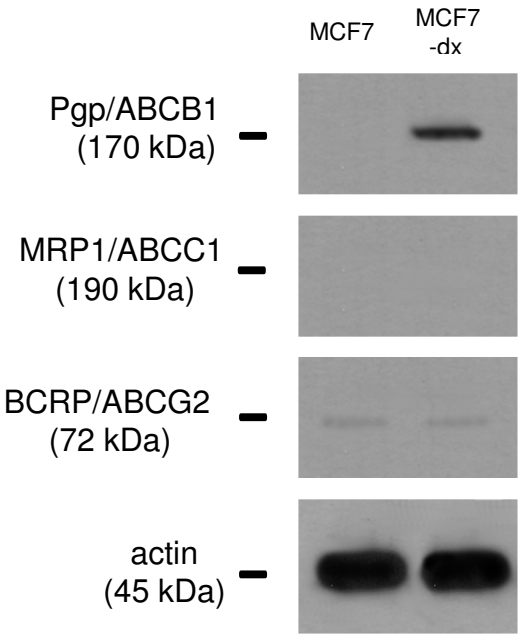

Supplementary Figure 2

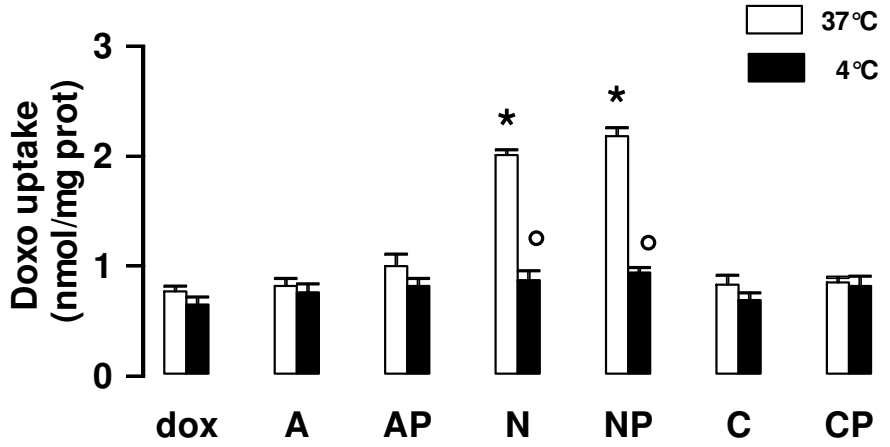

Supplementary Figure 3

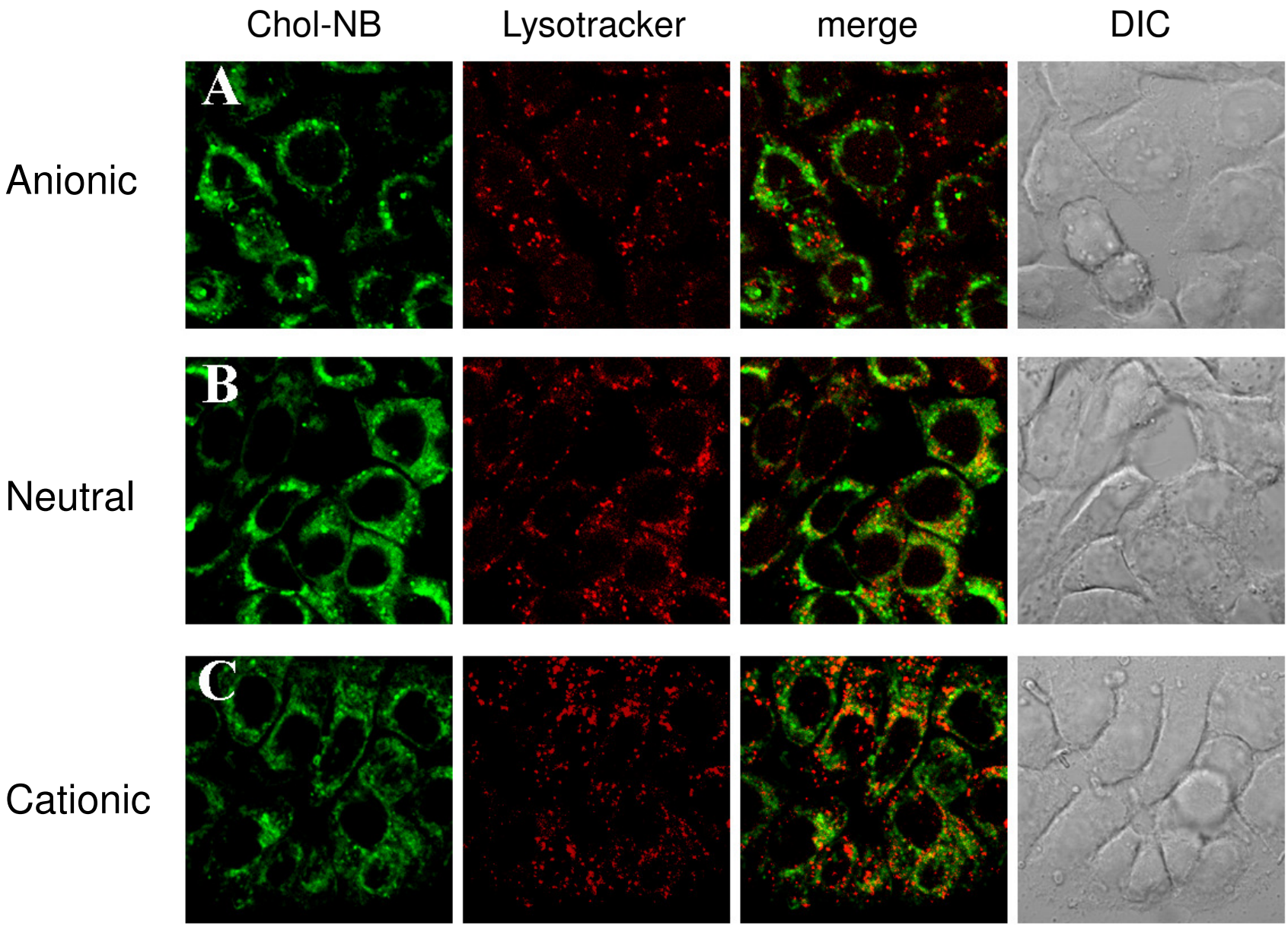

Supplementary Figure 4

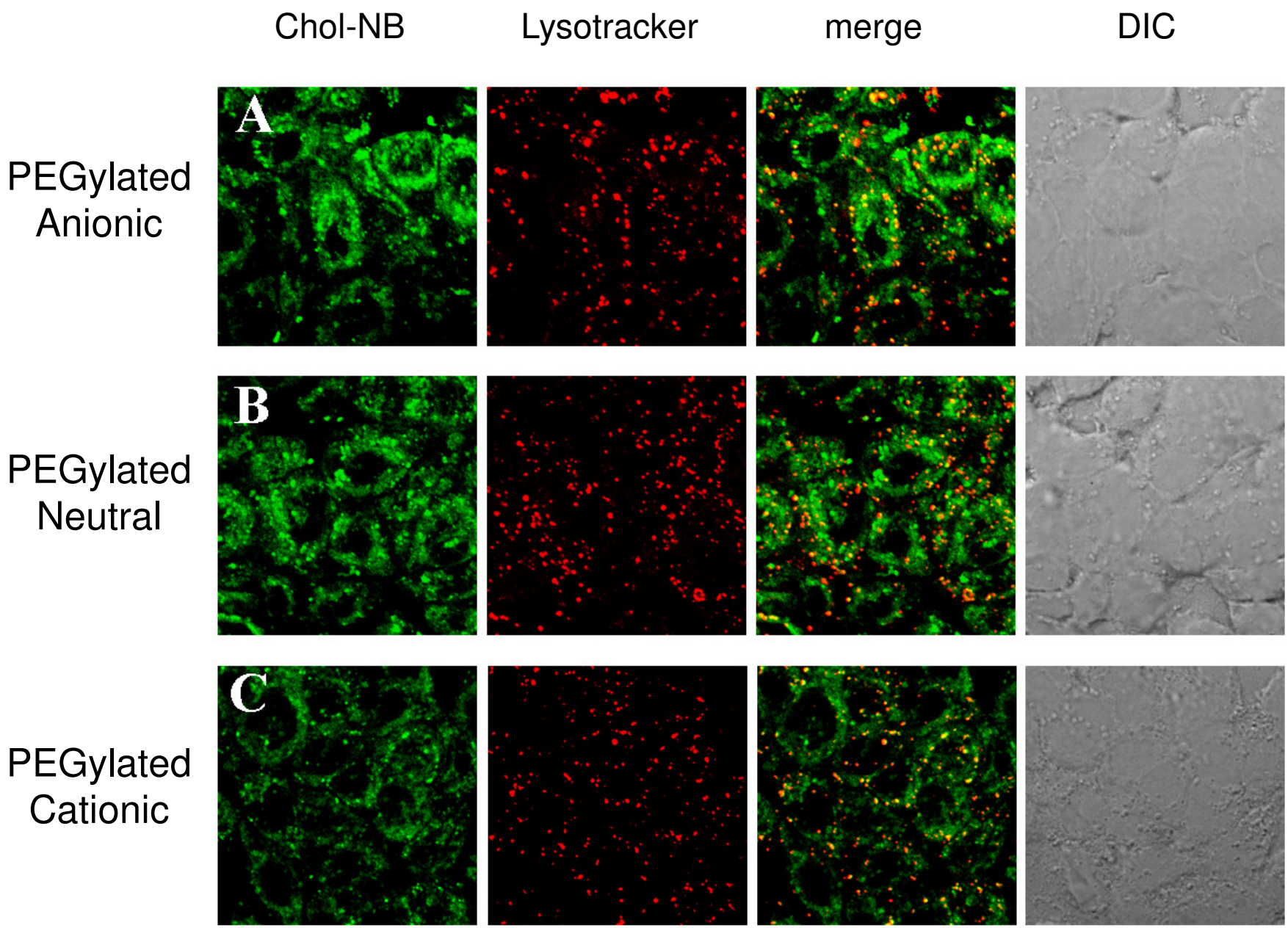

Supplementary Figure 5